

CRES

REMOTE SENSING LABORATORY



NASA CR-

144576

# RADAR RETURN FROM A CONTINUOUS VEGETATION CANOPY

Remote Sensing Laboratory  
RSL Technical Report 177-56

Thomas F. Bush  
Fawwaz T. Ulaby

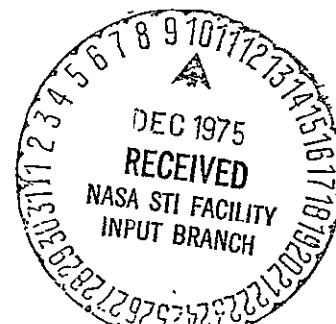
August, 1975

(NASA-CR-144576) RADAR RETURN FROM A	N76-12231
CONTINUOUS VEGETATION CANOPY. (Kansas Univ. Center for Research, Inc.) 61 p HC \$4.50 -	
CSCI 17I	Unclas
	G3/32 03906

Supported by:

NATIONAL AERONAUTICS AND SPACE ADMINISTRATION  
Lyndon B. Johnson Space Center  
Houston, Texas 77058

CONTRACT NAS 9-10261



THE UNIVERSITY OF KANSAS CENTER FOR RESEARCH, INC.

2291 Irving Hill Drive—Campus West Lawrence, Kansas 66045



THE UNIVERSITY OF KANSAS SPACE TECHNOLOGY CENTER

Raymond Nichols Hall

Center for Research, Inc.,

2291 Irving Hill Drive—Campus West Lawrence, Kansas 66045

Telephone: 913-864-4832

RADAR RETURN FROM A CONTINUOUS VEGETATION CANOPY

Remote Sensing Laboratory  
RSL Technical Report 177-56

Thomas F. Bush  
Fawwaz T. Ulaby

August, 1975

Supported by:  
NATIONAL AERONAUTICS AND SPACE ADMINISTRATION  
Lyndon B. Johnson Space Center  
Houston, Texas 77058  
CONTRACT NAS 9-10261

## TABLE OF CONTENTS

	<u>Page</u>
ABSTRACT . . . . .	i
1.0 INTRODUCTION . . . . .	1
2.0 SCATTEROMETER SYSTEM . . . . .	1
3.0 GROUND DATA ACQUISITION . . . . .	3
3.1 Soil Moisture . . . . .	3
3.2 Plant Moisture . . . . .	6
3.3 Plant Height . . . . .	6
4.0 CANOPY MODEL . . . . .	8
5.0 DATA PRESENTATION AND DISCUSSION . . . . .	11
5.1 Temporal Variations of $\sigma^{\circ}$ . . . . .	11
5.2 Implementation of the Canopy Model . . . . .	20
5.3 Angular Response of $\sigma^{\circ}$ . . . . .	28
5.4 Spectral Response of $\sigma^{\circ}$ . . . . .	39
6.0 CONCLUDING REMARKS . . . . .	39
REFERENCES . . . . .	45
APPENDIX A: Ground Truth Summary for 1974 Alfalfa Scattering Experiment	46
APPENDIX B: Alfalfa Scattering Coefficients, 1974 . . . . .	47

## LIST OF FIGURES

		<u>Page</u>
Figure 1.	Summarized ground truth data record for alfalfa, 1974.	5
Figure 2.	Diagram showing field locations of soil samples.	7
Figure 3.	Temporal variations of $\sigma^{\circ}$ measured at 8.6 GHz for angles of incidence of a) $0^{\circ}$ , b) $10^{\circ}$ , c) $40^{\circ}$ , and d) $70^{\circ}$ .	12
Figure 4.	Temporal variations of $\sigma^{\circ}$ measured at 13.0 GHz for angles of incidence of a) $0^{\circ}$ , b) $10^{\circ}$ , c) $40^{\circ}$ , and d) $70^{\circ}$ .	16
Figure 5.	Temporal variations of $\sigma^{\circ}$ measured at 17.0 GHz for angles of incidence of a) $0^{\circ}$ , b) $10^{\circ}$ , c) $40^{\circ}$ , and d) $70^{\circ}$ .	18
Figure 6.	Temporal variations of $\bar{\sigma}^{\circ}$ (the average value of $\sigma_{H}^{\circ}$ and $\sigma_{V}^{\circ}$ ) as measured at nadir with $\hat{\sigma}^{\circ}$ , the values predicted by the canopy model presented in section 4.0. Data are presented at a) 8.6 GHz, b) 13.0 GHz, and c) 17.0 GHz.	22
Figure 7.	Response of $\hat{\sigma}^{\circ}$ , the value of $\bar{\sigma}^{\circ}$ predicted by the canopy model, as a function of canopy height and soil moisture, $m_s$ . Curves are presented at a) 8.6 GHz, b) 13.0 GHz, and c) 17.0 GHz.	25
Figure 8.	Angular response of $\sigma^{\circ}$ of harvested alfalfa at 8.6 GHz ( $\sigma_{H}^{\circ}$ and $\sigma_{V}^{\circ}$ , 8a and 8b), 13.0 GHz ( $\sigma_{H}^{\circ}$ and $\sigma_{V}^{\circ}$ , 8c and 8d) and 17.0 GHz ( $\sigma_{H}^{\circ}$ and $\sigma_{V}^{\circ}$ , 8e and 8f). Note that both curves represent $\sigma^{\circ}$ of harvested alfalfa (11 cm and 17 cm) and that the values of the soil moistures were comparable but not identical.	29
Figure 9.	Angular response of $\sigma^{\circ}$ of two nearly mature stands of alfalfa at 8.6 GHz ( $\sigma_{H}^{\circ}$ and $\sigma_{V}^{\circ}$ , 9a and 9b), 13.0 GHz ( $\sigma_{H}^{\circ}$ and $\sigma_{V}^{\circ}$ , 9c and 9d), and 17.0 GHz ( $\sigma_{H}^{\circ}$ and $\sigma_{V}^{\circ}$ , 9e and 9f). Although the crops heights are practically identical, the measured values of soil moisture are quite different.	33

## LIST OF FIGURES

		Page
Figure 10.	Angular response of $\sigma^{\circ}$ of harvested and mature alfalfa at 8.6 GHz ( $\sigma_{H}^{\circ}$ and $\sigma_{V}^{\circ}$ , 10a and 10b), 13.0 GHz ( $\sigma_{H}^{\circ}$ and $\sigma_{V}^{\circ}$ , 10c and 10d), and 17.0 GHz ( $\sigma_{H}^{\circ}$ and $\sigma_{V}^{\circ}$ , 10e and 10f). Note the soil moistures which are nearly equal.	36
Figure 11.	Spectral response of $\sigma_{H}^{\circ}$ and $\sigma_{V}^{\circ}$ for two stands of alfalfa at different growth stages at $0^{\circ}$ (a and b), $30^{\circ}$ (c and d), $50^{\circ}$ (e and f), and $70^{\circ}$ (g and h).	40

## LIST OF TABLES

Table 1.	MAS 8-18 system specifications.	2
Table 2.	Number of spatially independent measurements with 90% confidence intervals of $\sigma^{\circ}$ (dB) of alfalfa.	4
Table 3.	Estimated values of the regression constants as a function of frequency for the proposed canopy model of $\sigma^{\circ}$ .	21

## ABSTRACT

The radar backscatter coefficient,  $\sigma^{\circ}$ , of alfalfa was investigated as a function of both radar parameters and the physical characteristics of the alfalfa canopy. Measurements were acquired with an 8-18 GHz FM-CW mobile radar over an angular range of  $0^{\circ}$ - $70^{\circ}$  as measured from nadir. The experimental data indicates that the excursions of  $\sigma^{\circ}$  at nadir cover a range of nearly 18 dB during one complete growing cycle. An empirical model for  $\sigma^{\circ}$  was developed which accounts for its variability in terms of soil moisture, plant moisture and plant height.

## 1.0 INTRODUCTION

Critical to the successful application of radar remote sensing techniques to agricultural land use mapping is the understanding of the dependence of the backscattering coefficient  $\sigma^0$  of a vegetated scene on the geometrical and electrical properties of the remotely sensed scene. Establishing these relationships requires a) the acquisition of backscatter data over a wide range of the measurable target parameters and b) the construction of theoretical and/or empirical models (based on the measured data) from which in-depth inferences can be made on the target-signal interaction process. Moreover, since the desired relationships are often a function of the signal parameters (frequency, polarization and incidence angle), it is important that the data collection and modeling be made over as wide a range of the signal parameters as is practically feasible with present day sensors.

This study presents the results of an investigation conducted to determine the microwave backscattering properties of a continuous vegetation canopy over the 8-18 GHz frequency region (3.75 - 1.67 cm in wavelength). Using a truck-mounted radar spectrometer, measurements were acquired from an alfalfa field at angles of incidence ranging from nadir ( $0^\circ$ ) to  $70^\circ$  for horizontal transmit-horizontal receive (HH) and vertical transmit-vertical receive (VV) polarization configurations. As a perennial crop, alfalfa is usually harvested three or often four times per year; upon reaching a height of 50-70 cm, it is cut, dried and baled, and then allowed to grow again. During the 1974 summer season radar observations were made over two complete growing cycles of alfalfa.

## 2.0 SCATTEROMETER SYSTEM

The scatterometer employed in collecting the data used in this study is the 8-18 GHz Microwave Active Spectrometer (MAS 8-18) [1]. This is a mobile, truck-mounted system capable of making scattering measurements at 11 frequencies in its 8-18 GHz range. It employs a dual antenna system configured to allow both horizontal-transmit horizontal-receive (HH) and vertical-transmit vertical-receive (VV) modes of operation. Measurements can be made at angles of incidence between  $0^\circ$  (nadir) and  $70^\circ$ . Table 1 presents the system specifications pertinent to the discussion of this experiment.

TABLE 1.  
MAS 8-18 System Specifications

Type	FM-CW
Modulating Waveform	Triangular
Frequency Range	8-18 GHz
FM sweep: $\Delta f$	800 MHz
Transmitter Power	10 dBm (10 mW)
Intermediate Frequency	50 kHz
IF Bandwidth	10.0 kHz
Antennas	
Height above ground	26 m
Reflector diameter	61 cm
Feeds	Cavity backed, log-periodic
Polarization	Horizontal transmit-Horizontal receive (HH) Vertical transmit-Vertical receive (VV)
Incidence Angle Range	$0^{\circ}$ (nadir)- $80^{\circ}$
Calibration:	
Internal	Delay Line
External	Luneberg Lens



Being a wide band radar the MAS 8-18 provided fading reduction by averaging samples of the return signal energy over its 800 MHz bandwidth. Due to the limited extent of the resolution cell area, frequency averaging would not provide the fading reduction necessary for the data precision and accuracy desired. Thus spatial averaging was also employed.

The number of independent samples of return power averaged in the frequency domain can be determined through the knowledge of the target extent measured radially from the radar antenna [2]. For this experiment however, the target height, and thus the radial target extent changed as the vegetation canopy matured. For this reason a worst case approach was taken by assuming that no penetration of the radar signal into the vegetation canopy occurred. This assumption and a knowledge of the number of spatially independent measurements collected allow the estimation of confidence intervals for  $\sigma^{\circ}$ . Ninety per cent confidence intervals for  $\sigma^{\circ}$  of alfalfa are presented in Table 2. Since these confidence intervals are based on a zero penetration assumption, under most conditions the confidence intervals associated with the measured data will most likely be narrower than those shown in Table 2.

### 3.0 GROUND DATA ACQUISITION

Because the methods of collecting and processing the ground "truth" data acquired in support of the scattering measurements have been previously discussed by Cihlar [3], only a short description of the processing methods used and a summary of the results obtained will be presented. Figure 1 provides, in a summarized fashion, a time history of the pertinent target characteristics with a more complete ground data record being available in Appendix A.

#### 3.1 Soil Moisture

A recent report by Cihlar and Ulaby [4] reviews the dielectric properties of various soil types as a function of their physical properties. Of the conclusions reached it was noted that soil moisture played the overwhelming role in determining the complex

Table 2. Number of Spatially Independent Measurements  
with 90% Confidence Intervals of  $\sigma^{\circ}$  (dB) of Alfalfa

Incidence Angle	Number of Spatially Independent Measurements	90% Confidence Intervals (dB)
0°	18	+1.8 -2.0
10°	17	+1.8 -2.0
20°	16	+1.0 -1.3
30°	15	+0.9 -1.0
40°	14	+0.8 -0.8
50°	13	+0.7 -0.7
60°	13	+0.4 -0.4
70°	13	+0.3 -0.3

5

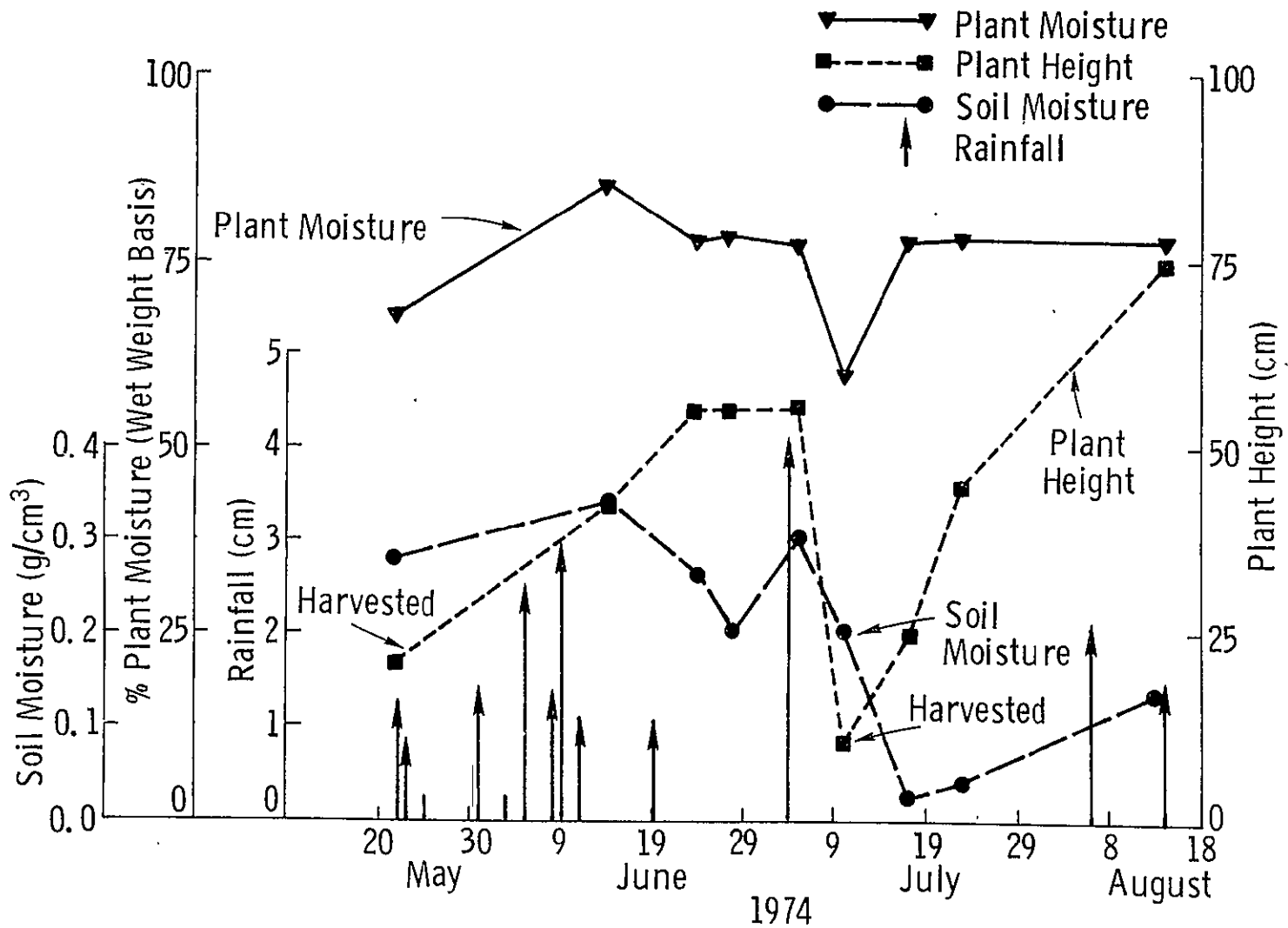


Figure 1. Summarized ground truth data record for alfalfa, 1974.

dielectric constant of the soil. In turn the dielectric properties of the soil are reflected in  $\sigma^{\circ}$ . To aid in determining the relationship between  $\sigma^{\circ}$  and soil moisture content, soil samples were collected at the time of each scattering measurement. Figure 2 indicates the locations within the test field where soil samples were collected. The location of each pair of sampling points was chosen so that locations #1, #2 and #3 approximately corresponded to scattering measurements made within the angular ranges of  $0^{\circ}$ - $20^{\circ}$ ,  $30^{\circ}$ - $50^{\circ}$  and  $60^{\circ}$ - $70^{\circ}$  respectively. After recording the sample weight, they were dried in an oven and again weighed so that the gravimetric soil moisture content could be determined. The measured values of the soil moisture content were then averaged in a pair-wise manner and converted to volumetric soil moisture content using the soil bulk density as the conversion factor. Thus all soil moisture contents reported herein, designated as  $m_s$ , are expressed in units of  $\text{g}/\text{cm}^3$ . Due to skin depth considerations [4] only the top 2 cm samples were used in the analyses. Subsequent analyses involving  $m_s$  will make use of the soil sample location and incidence angle correspondence. For example to determine the effects of  $m_s$  on  $\sigma^{\circ}$  as measured at a  $40^{\circ}$  angle of incidence,  $m_s$  as measured at location #2 would be used as the independent variable in the analysis. Figure 1 shows the variations of  $m_s$  at location #2 as a function of time.

### 3.2 Plant Moisture

As with soil moisture, plant moisture has been shown to significantly influence the dielectric properties of vegetation [5]. Thus, as part of the scattering experiment, a number of alfalfa plant samples were collected at the time a scattering measurement was made. These samples were processed so that the plant moisture content,  $m_p$ , as measured on a wet weight basis was obtained. Figure 1 presents the results of this analysis. It should be noted that the variations of  $m_p$  as a function of time were somewhat small except for the July 10 value of 0.6 which was measured shortly after the alfalfa was harvested.

### 3.3 Plant Height

In addition to the above parameters, the time history of the average height of the vegetation canopy was also recorded (Figure 1). It should be noted that the alfalfa completed two growth cycles during the observation period. The reader should bear in mind that while plant height is certainly one indicator of plant maturity there are a variety of physiological phenomena occurring during the maturation process.

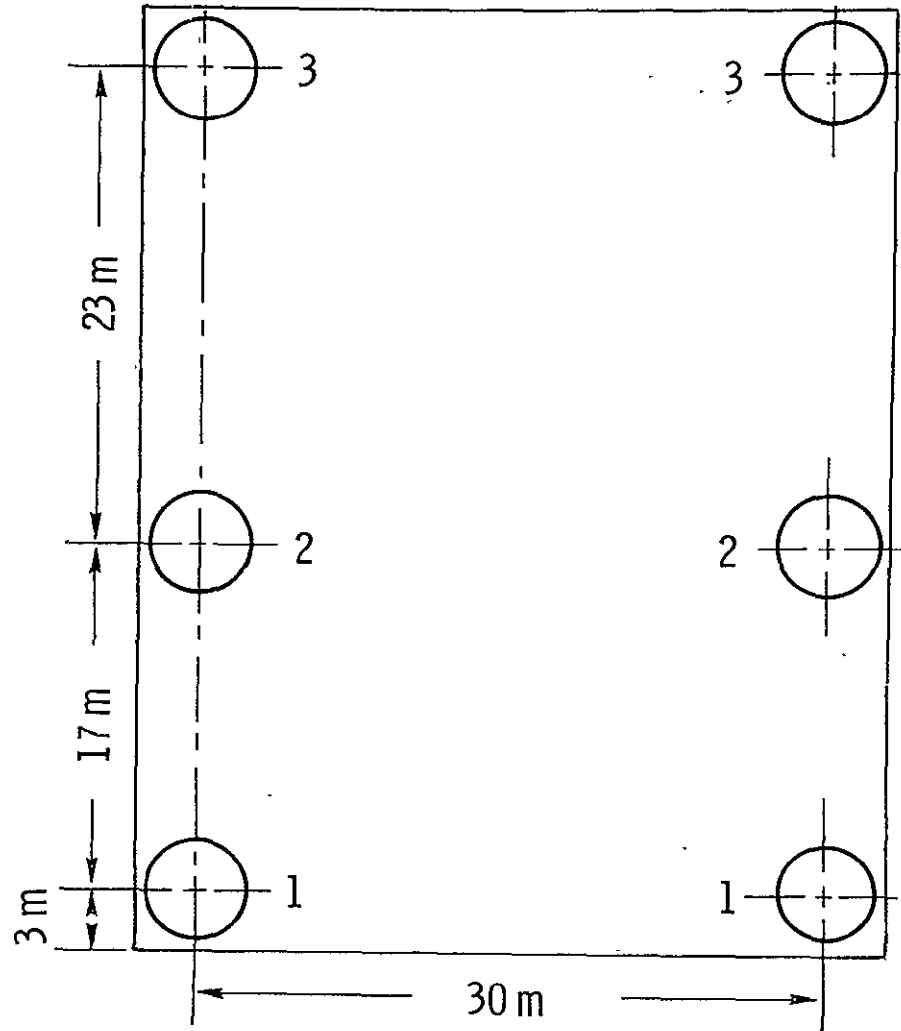


Figure 2. Diagram showing field locations of soil samples.

#### 4.0 CANOPY MODEL

If we consider the alfalfa canopy as a lossy dielectric layer between the air and soil media, then in general, the backscattered return would be composed of contributions by the canopy itself and contributions by the underlying soil. In the absence of vegetation cover, the bare soil backscattering coefficient  $\sigma_{bs}^0$  expressed in dB was found to vary linearly with soil moisture content  $m_s$  [6] which suggests an exponential variation if  $\sigma_{bs}^0$  is expressed in real units:

$$\sigma_{bs}^0 = A \exp(B \cdot m_s) \quad (1)$$

where A and B are constants for a given set of the sensor parameters and the soil surface roughness.

Vegetation is a dynamic target; over a growing cycle several plant parameters of interest can vary. Aside from "shape" variations, these parameters include plant height  $h$ , the bulk density of the vegetation canopy  $\rho$ , and plant moisture content  $m_p$ . Measurements of the dielectric constant of plant leaves by Carlson [5] at 8.5 GHz indicate a strong dependence on moisture content. Based on data from corn, grass and taxus samples, he proposed the following approximate formula:

$$\epsilon_p = \epsilon'_p - j\epsilon''_p = 1.5 + \left( \frac{\epsilon'_w}{2} - j \frac{\epsilon''_w}{3} \right) m_p \quad (2)$$

where  $\epsilon'$  and  $\epsilon''$  are the real and imaginary parts of the relative dielectric constant,  $m_p$  is the fractional amount of moisture present in the vegetation (on a wet weight basis) and the subscripts p and w refer to plant and water respectively. From (2) the loss tangent is given by:

$$\tan \delta_p = \frac{\epsilon''_p}{\epsilon'_p} = \frac{\epsilon''_w m_p}{4.5 + 1.5\epsilon'_w m_p} \quad (3)$$

At an air temperature of 30°C, typical of the environmental conditions under which the data reported in this paper were acquired,  $(\epsilon'_w, \epsilon''_w)$  vary between (68.0, 23.8) at 8 GHz and (46.8, 35.6) at 18 GHz [7]. Over two growth cycles of alfalfa, the smallest measured value of  $m_p$  was 0.6 corresponding to the cut alfalfa and the largest value was 0.85 (Figure 1). In view of the values of  $\epsilon'_w$  and  $m_p$ , neglecting the constant term of 4.5 in the denominator of (3) amounts to less than 10% error in the worst case. Hence,

$$\tan \delta_p \approx \frac{2}{3} \frac{\epsilon''_w}{\epsilon'_w} \quad (4)$$

which is independent of  $m_p$ . Moreover, at a given frequency and in the absence of wide variations in the physical temperature of the plant,  $\tan \delta_p$  is approximately a constant.

The attenuation suffered by a wave propagating through a vegetated medium is in general caused by scattering and by absorption losses. In view of the difficulty encountered in accounting for the loss term due to scattering, it will be assumed herein that as a first order approximation, the absorption loss is the dominant term. The justification for making this assumption is borne out by the close fit between the expression derived on this basis and the experimental results of  $\sigma^0$  at nadir (section 5.2). Neglecting the scattering-loss term is, in effect, equivalent to assuming that the vegetation medium is homogeneous.

The attenuation coefficient of a homogeneous medium of dielectric constant  $\epsilon_p$  is given by:

$$\alpha_p = \frac{2\pi}{\lambda} \left[ \frac{\epsilon'_p}{2} \left[ (1 + \tan^2 \delta_p)^{1/2} - 1 \right] \right]^{1/2} \quad (5)$$

nepers/m, with the wavelength  $\lambda$  expressed in meters. Applying the same approximation for  $\epsilon'_p$  used in deriving (4), the attenuation coefficient dependence on  $m_p$  becomes:

$$\alpha_p = k_1 m_p^{1/2} \quad (6)$$

where

$$k_1 = \frac{\pi}{\lambda} \left[ \epsilon'_w \left[ (1 + \tan^2 \delta_p)^{1/2} - 1 \right] \right]^{1/2} \quad (7)$$

which is only frequency and temperature dependent. To account for the fact that the canopy is not a homogeneous layer consisting entirely of plants, but instead is mostly air, the effective canopy attenuation coefficient is defined by:

$$\alpha_c = \rho k_1 m_p^{1/2} \quad (8)$$

where  $\rho$  is the bulk density of the vegetation. For most crops  $\rho$  is a function of height  $h$ ; with alfalfa, as the plants grow taller they also get denser, thereby suggesting that  $\rho$  is an increasing function of  $h$ . In the absence of experimental values for  $\rho$ , the following dependence is suggested:

$$\rho(h) = k_2 h^x \quad (9)$$

where  $k_2$  is a constant and  $x$  is a positive exponent to be determined empirically (section 5.2). Assuming that for a given height  $h$ , the canopy is approximately homogeneous, the total roundtrip power attenuation at nadir is then given by:

$$\Gamma(h, m_p) = 4 \alpha_c h \quad (10)$$

$$= 4 k_1 k_2 m_p^{1/2} h^{x+1}$$

$$= C m_p^{1/2} h^y \quad (11)$$

where  $C = 4 k_1 k_2$  and  $y = x + 1$ . At angles other than nadir, (11) should be modified to account for path length. Neglecting reflection at the canopy-air interface, the soil contribution to the measured backscattering coefficient by the vegetation-covered soil is from (1) and (11):

$$\sigma_{cs}^o = A \exp(B m_s - \Gamma)$$

$$= A \exp(B m_s - C m_p^{1/2} h^y) \quad (12)$$

In addition to attenuating the soil component, the canopy contributes a backscattering coefficient of its own,  $\sigma_c^o$ . Since the backscatter from a target is influenced by its dielectric properties and geometry, and due to the lack of an appropriate theory capable of incorporating these parameters, it is suggested here that  $\sigma_c^o$  take a form similar to that of  $\Gamma$ :

$$\sigma_c^o = D m_p^{1/2} h^z \quad (13)$$



where  $D$  and  $z$  are constants. The rationale behind the above formulation is that the total attenuation of a lossy medium is closely related to the medium emissivity which in turn is related to its scattering properties [8]. Combining (12) and (13), the total scattering coefficient of the canopy (above the soil) is:

$$\begin{aligned}\sigma^{\circ} &= \sigma_{cs}^{\circ} + \sigma_c^{\circ} \\ &= A \exp(B m_s - C m_p^{1/2} h^y) + D m_p^{1/2} h^z\end{aligned}\quad (14)$$

The application of the above model to the measured data (section 5.2) provides the best agreement between theory and experiment at nadir. The empirically determined values of  $y$  and  $z$  are 2.6 and 1.0, respectively.

## 5.0 DATA PRESENTATION AND DISCUSSION

### 5.1 Temporal Variations of $\sigma^{\circ}$

Figures 3a-d present temporal variations of the measured value of  $\sigma^{\circ}$ , the back-scattering coefficient, at 8.6 GHz. Both  $\sigma_H^{\circ}$  and  $\sigma_V^{\circ}$  are shown at four angles of incidence,  $0^{\circ}$  (3a),  $10^{\circ}$  (3b),  $40^{\circ}$  (3c) and  $70^{\circ}$  (3d). (Complete data are presented in Appendix B). An initial inspection of Figure 3a indicates that the dynamic range of  $\sigma^{\circ}$  (at 8.6 GHz,  $0^{\circ}$ ) during the observation period was nearly 18 dB, implying that indeed the radar responded to the physical variations of the alfalfa as it completed two growth cycles. Two distinct maxima and minima are also noted. The maxima occur on May 22 and July 10 and the minima, while not quite as pronounced, occur near June 28 and August 1. From Figure 1 it is found that the maxima coincide exactly with the days on which the harvested alfalfa was observed. Furthermore the minima correspond to those time periods during which the alfalfa reached maximum height. In fact it is noted that throughout the observation period  $\sigma_H^{\circ}$  and  $\sigma_V^{\circ}$  are roughly inversely related to plant height (Figure 1).

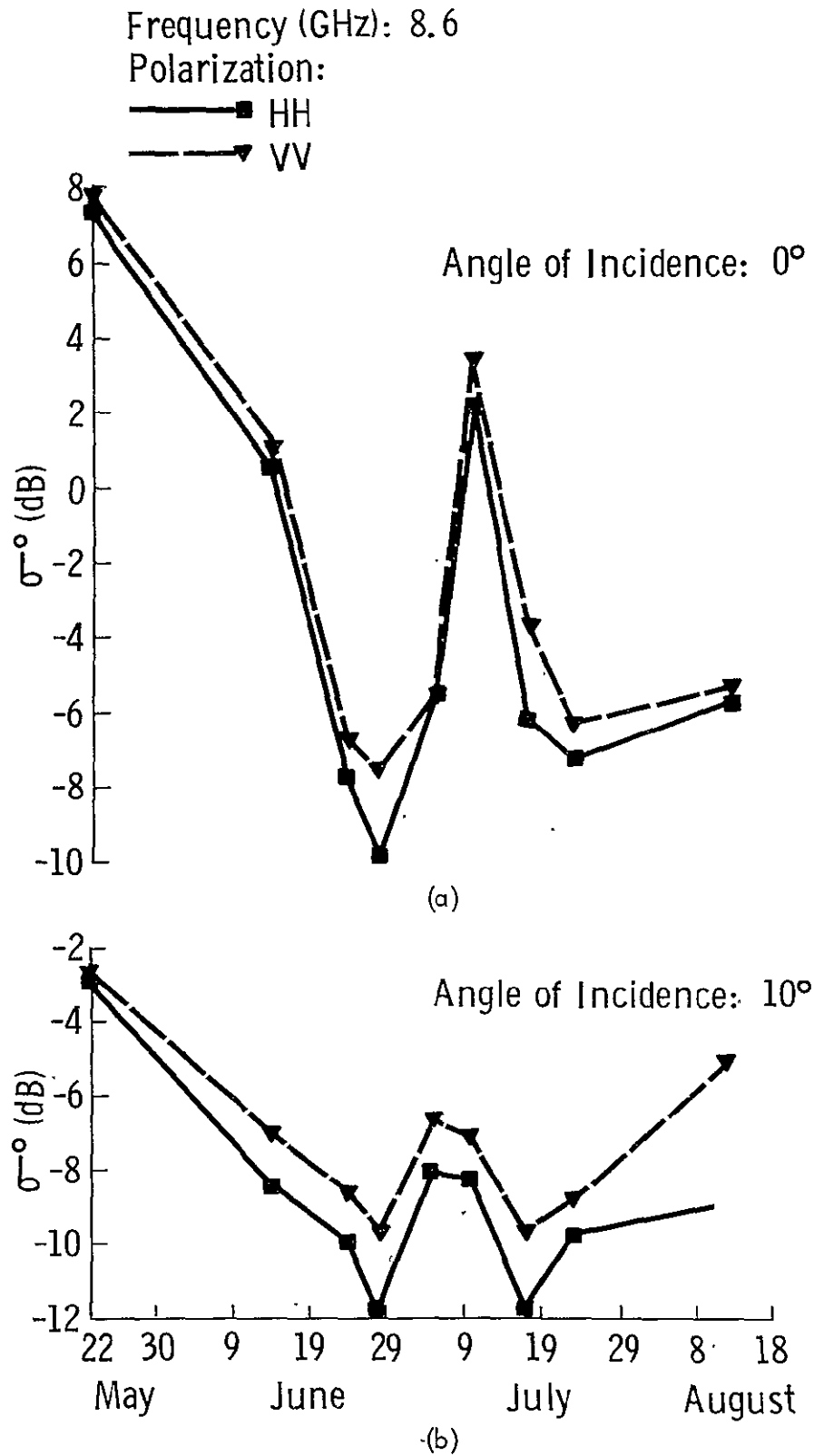


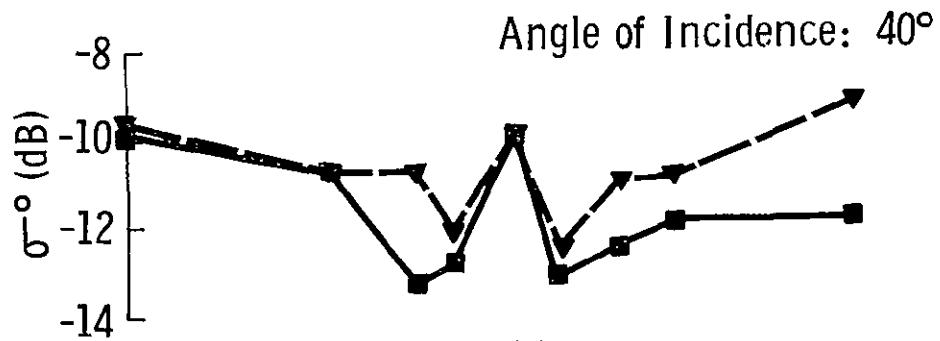
Figure 3. Temporal variations of  $\sigma^0$  measured at 8.6 GHz for angles of incidence of a) 0°, b) 10°, c) 40°, and d) 70°.

Frequency (GHz): 8.6

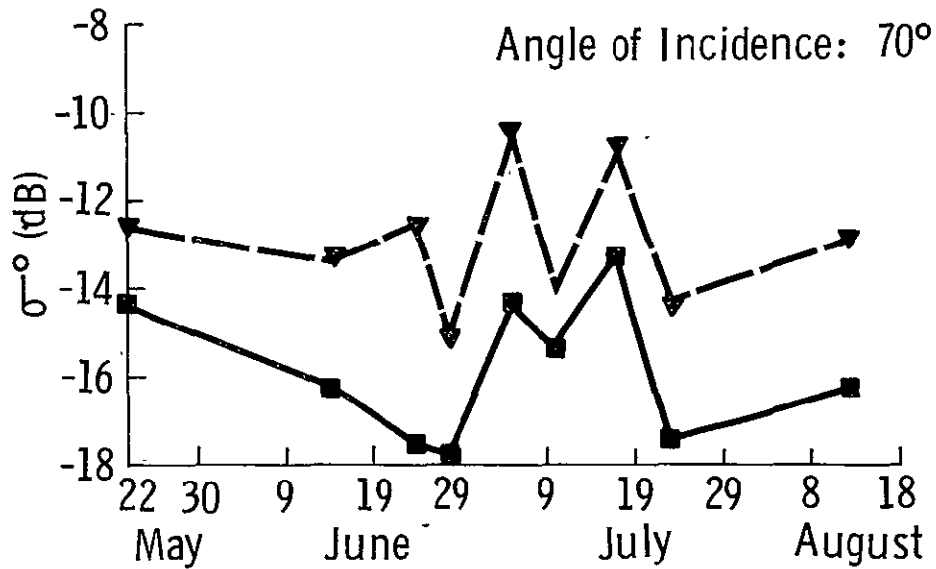
Polarization:

—■— HH

- - -▼- - VV



(c)



(d)

In an earlier report [9] discussing 4-8 GHz backscatter data from alfalfa it was suggested that of the total radar return from mature alfalfa, backscatter from the alfalfa alone dominated the return with a relatively small contribution from the underlying soil. Again this seems to be a partial explanation for the behavior of the  $\sigma^0$  versus time curve presented in Figure 3a. Consider the target as two media; the first being the vegetation canopy while the second being the underlying soil. Because alfalfa is a perennial crop the underlying soil is left uncultivated for four or perhaps more years. Due to the action of natural erosive elements (rain, wind, etc.) the soil assumes a quite smooth character. Such was the character of the soil during the observation period under discussion. Thus when a backscatter measurement is made of a short stand of alfalfa at nadir the radar will "see" the smooth soil surface causing a relatively large amount of the incident energy to be reflected back to the radar. As the alfalfa matures however, both the plant height and density increase causing the loss within the canopy to increase. This attenuation will result in a masking of the contributions by the underlying soil. Certainly the return from the vegetation canopy will increase as the canopy height and density increase but it is felt that this effect will not be large enough to balance the reduction in the return from the soil. Perhaps this can be more easily seen by an observation of  $\sigma^0$  as measured on June 14 and July 23. From Figure 1 we note that while the crop heights were nearly equal, (about 44 cm) the earlier value of  $\sigma^0$  was measured when  $m_s$ , the soil moisture, was about  $0.34 \text{ g/cm}^3$  in contrast to  $0.04 \text{ g/cm}^3$  as recorded on July 23. From Figure 3a we note that  $\sigma_H^0$  as measured on June 14 was about 7.5 dB higher than  $\sigma_H^0$  on July 23, indicating that soil moisture can have an effect on  $\sigma^0$  of alfalfa at nadir.

Next consider data collected on May 22 and June 24. In this case the soil moisture contents were very similar ( $0.28 \text{ g/cm}^3$  on 5/22 and  $0.26 \text{ g/cm}^3$  on 6/24) while the alfalfa on May 22 was only 17 cm tall as contrasted with the 55 cm tall alfalfa measured on June 24. Again from Figure 3a we can note the effect of this change in crop height and density to be that of decreasing  $\sigma_H^0$  from about 7 dB on May 22 to a value of about -8 dB on June 24. Thus it appears that at nadir the radar backscatter from mature alfalfa is generally dominated by scatter from the plant canopy while the return from short and/or immature alfalfa is strongly dependent on soil moisture.

Figure 3b presents  $\sigma^{\circ}$  as a function of time for an angle of incidence of  $10^{\circ}$ . An immediate and dramatic change in the trends of  $\sigma^{\circ}$  is noted. Perhaps most notable is the lack of a maximum on July 10. Moreover the dynamic range of  $\sigma^{\circ}$  has also been reduced to 9 dB, which (in real units) is about 12% of the observed dynamic range at  $0^{\circ}$ . Furthermore there does not appear to be as strong a dependence of  $\sigma^{\circ}$  on height as was noted earlier for the nadir data. Figures 3c and 3d present data collected at 8.6 GHz at  $40^{\circ}$  and  $70^{\circ}$  respectively. Again no strong dependence of  $\sigma^{\circ}$  on the measured target variables is noted although the  $10^{\circ}$  and  $40^{\circ}$  data bear certain similarities.

Figures 4a-d present the temporal variations of  $\sigma^{\circ}$  as measured at 13.0 GHz. It is immediately apparent that the trends observed at 8.6 GHz at a  $0^{\circ}$  angle of incidence are present at 13.0 GHz. While there are certain shifts in the absolute levels of  $\sigma^{\circ}$  as measured at 8.6 and 13.0 GHz, the maxima and minima still persist at identical points in time. At  $10^{\circ}$ , 13.0 GHz (Figure 4b) the contrast with the  $0^{\circ}$  data is again noted. Furthermore there are no definite consistencies between the  $10^{\circ}$  data as measured at 8.6 GHz (Figure 3b) and 13.0 GHz (Figure 4b) or between the response of  $\sigma_{H}^{\circ}$  and  $\sigma_{V}^{\circ}$  as measured at 13.0 GHz. At  $40^{\circ}$  and  $70^{\circ}$ , Figures 4c and 4d, the response of  $\sigma^{\circ}$  to the passage of time is very similar to  $\sigma^{\circ}$  as measured at 8.6 GHz at corresponding angles of incidence. It is interesting to note that the dynamic range of  $\sigma_{V}^{\circ}$  at 13.0 GHz,  $40^{\circ}$  is only 2.8 dB, indicating very little dependence of  $\sigma^{\circ}$  on the various crop characteristics under consideration.

Finally, 17.0 GHz data are presented in Figures 5a-d. The trends at  $0^{\circ}$ , Figure 5a, are certainly consistent with the previous observations at 8.6 and 13.0 GHz. Again the  $10^{\circ}$  data, Figure 5b, show no consistent variation when compared to the 8.6 or 13.0 GHz  $10^{\circ}$  data. The  $40^{\circ}$  and  $70^{\circ}$  data (Figures 5c and 5d) however show responses very similar to those observed at the lower frequencies at corresponding angles of incidence. Although differences between  $\sigma_{H}^{\circ}$  and  $\sigma_{V}^{\circ}$  will be discussed in section 5.3, it should be noted that all the data discussed so far have displayed a consistent tendency for  $\sigma_{V}^{\circ}$  to be higher than  $\sigma_{H}^{\circ}$  at angles other than  $0^{\circ}$ . Furthermore it is noted that at all angles other than  $10^{\circ}$ ,  $\sigma_{H}^{\circ}$  and  $\sigma_{V}^{\circ}$  have displayed trends very similar, if not nearly identical, to one another.

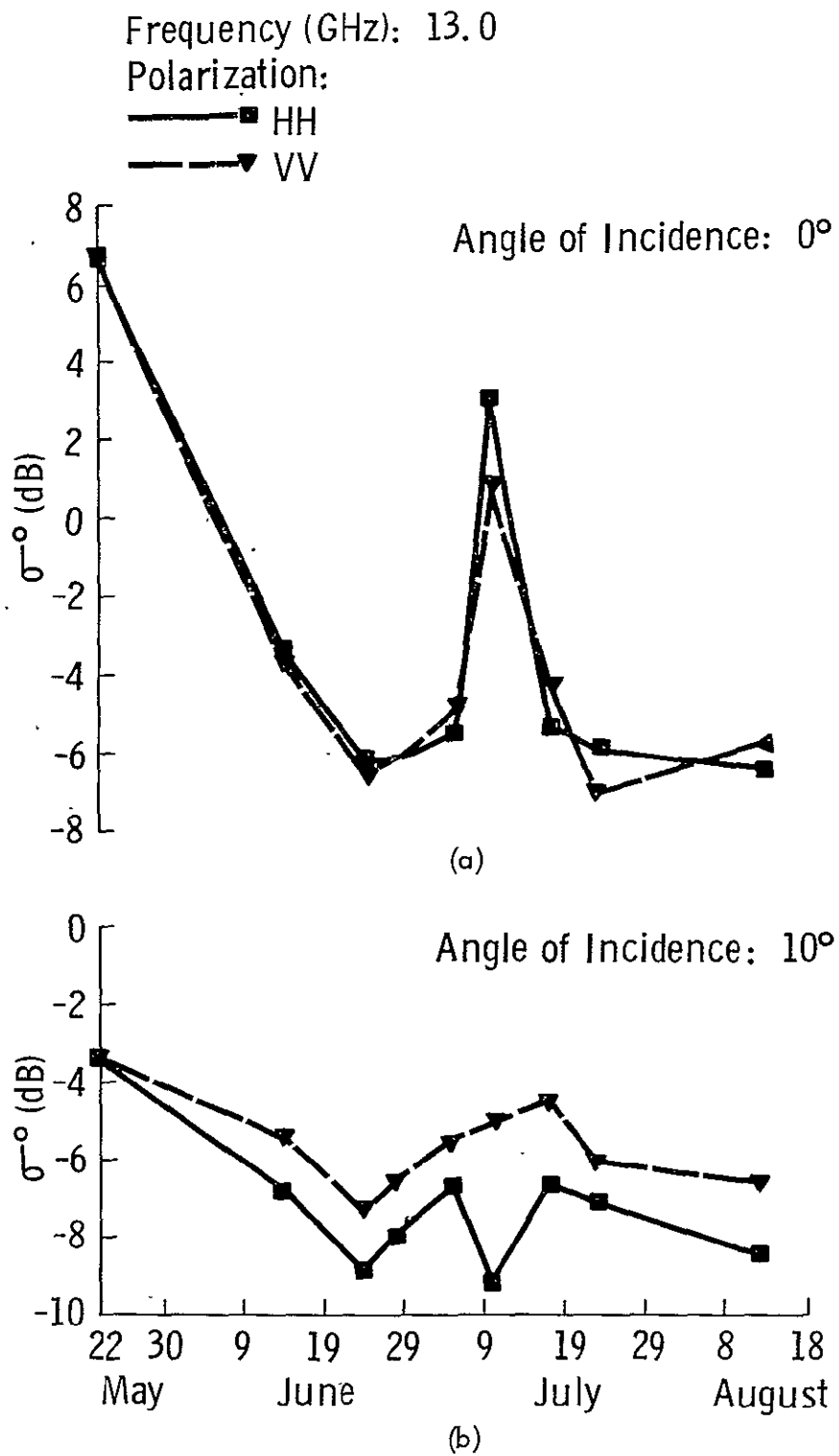


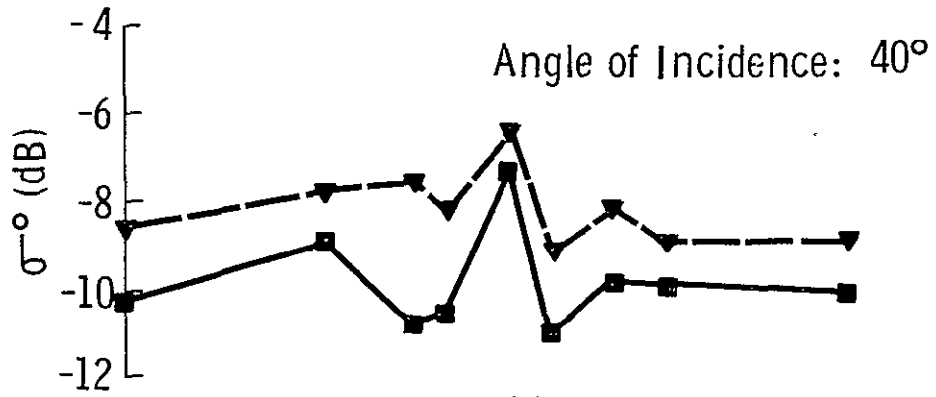
Figure 4. Temporal variations of  $\sigma_0^0$  measured at 13.0 GHz for angles of incidence of a) 0°, b) 10°, c) 40°, and d) 70°.

Frequency (GHz) 13.0

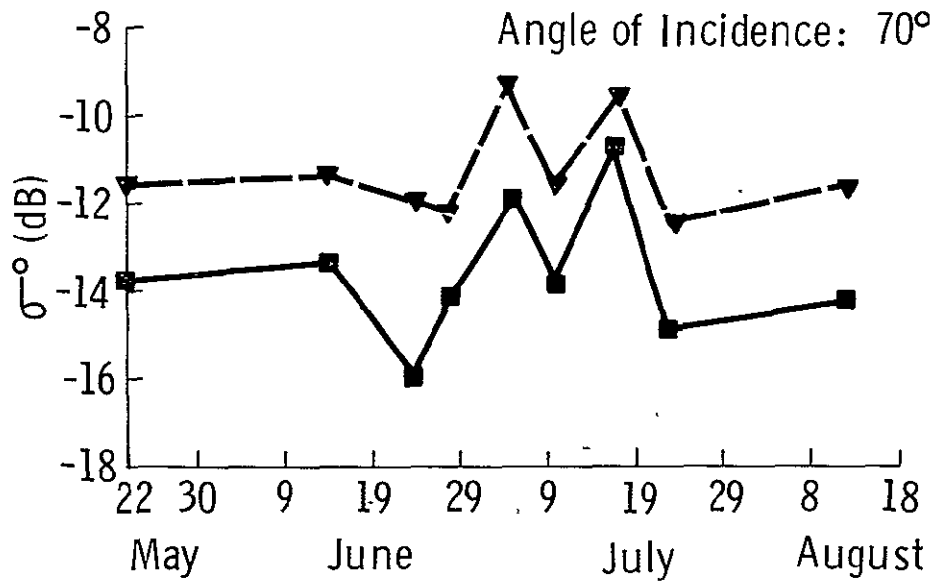
Polarization:

—■— HH

- - -▼- - VV



(c)



(d)

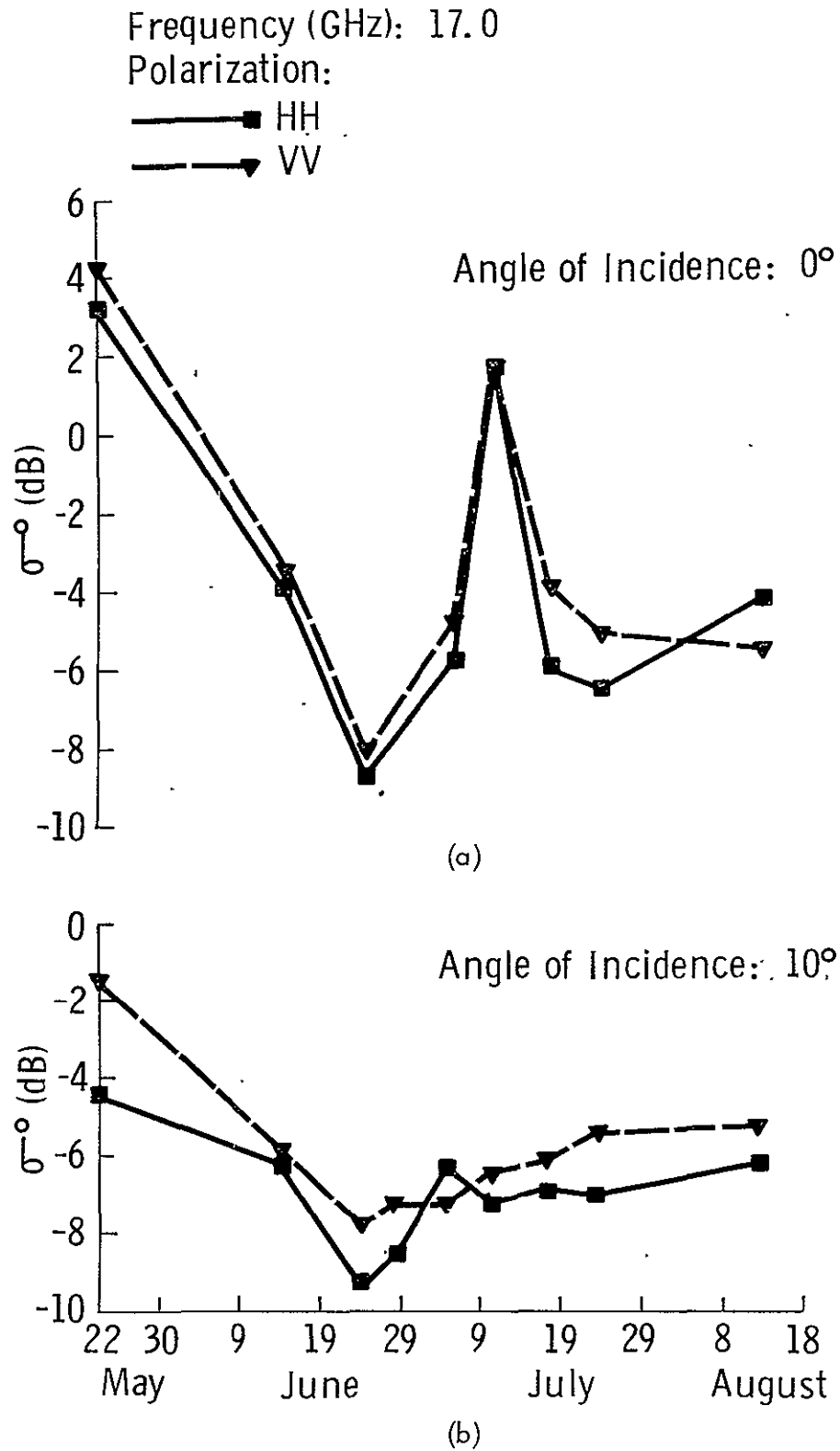


Figure 5. Temporal variations of  $\sigma_0^\theta$  measured at 17.0 GHz for angles of incidence of a) 0°, b) 10°, c) 40°, and d) 70°.

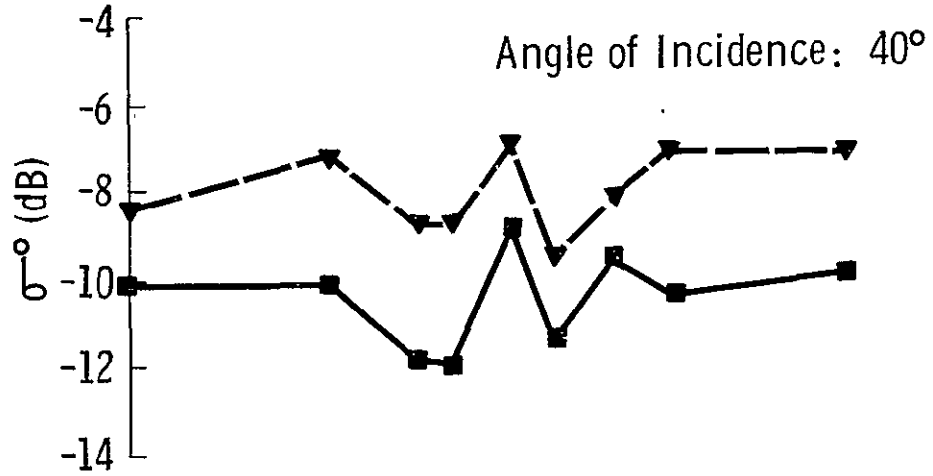


Frequency (GHz): 17.0

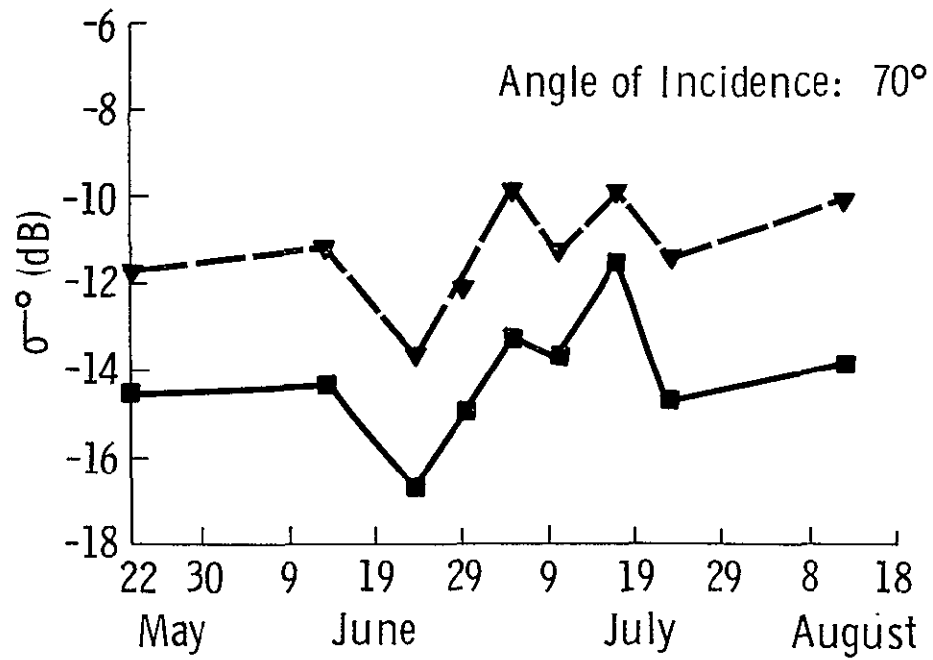
Polarization:

—■— HH

- - -▲- - VV



(c)



(d)

## 5.2 Implementation of the Canopy Model

Having discussed the temporal variations of  $\sigma^{\circ}$ , this section of the report will discuss the estimation of the regression constants A, B, C and D as defined in the canopy model proposed in section 4.0 and the results of the model predictions. To estimate the values of the above regression constants the nonlinear regression program BMDP3R\* which obtains a minimum mean squared error fit to a given set of data, was employed. To reduce the effects of fading in the measured values of  $\sigma^{\circ}$  at nadir,  $\sigma_{\text{H}}^{\circ}$  and  $\sigma_{\text{V}}^{\circ}$  were averaged. Because alfalfa is a continuous canopy target it is felt that there should be no significant polarization effects in  $\sigma^{\circ}$  at nadir. This average value of  $\sigma^{\circ}$  will be denoted as  $\bar{\sigma}^{\circ}$ . At each frequency, the values of A, B, C and D were estimated as described above, with the results of these regression analyses presented in Table 3. Making use of these results, Figures 6a-c present  $\bar{\sigma}^{\circ}$ , the average value of  $\sigma_{\text{H}}^{\circ}$  and  $\sigma_{\text{V}}^{\circ}$ , and  $\hat{\sigma}^{\circ}$ , the value predicted by the appropriate regression equation. Only the results of the analyses at 8.6, 13.0 and 17.0 GHz are presented in these figures. Note that  $\hat{\sigma}^{\circ}$  predicts  $\bar{\sigma}^{\circ}$  reasonably well, particularly for the higher values of  $\bar{\sigma}^{\circ}$ .

Making use of the canopy model it is possible to estimate the behavior of  $\bar{\sigma}^{\circ}$  as a function of the various target characteristics. Figures 7a-c present curves of  $\hat{\sigma}^{\circ}$  as a function of crop height for various values of  $m_s$ , the soil moisture content. Figure 7a, representing  $\hat{\sigma}^{\circ}$  at 8.6 GHz, clearly indicates the dependence of  $\sigma^{\circ}$  on soil moisture and crop height. If an average height of 0.35 meters is chosen, for example, it is noted that  $\hat{\sigma}^{\circ}$  can range between -7.0 dB and +3.0 dB for a range of  $m_s$  between 0.0 and 0.30 g/cm<sup>3</sup>, respectively. If we chose a value of h of 0.60 meters however, the range over which  $\hat{\sigma}^{\circ}$  varies for the same 0.30 g/cm<sup>3</sup> range of  $m_s$  is only about 1.0 dB. Choosing a value of  $m_s$  of 0.0 it is seen that the effect of a 0.70 meter increase in height causes  $\hat{\sigma}^{\circ}$  to vary within a 4.6 dB range with a minimum occurring around a value of h = 0.5 meters. For h < 0.5 m, the exponentially decaying shape of the  $\hat{\sigma}^{\circ}$  curve indicates that the canopy is acting primarily as an attenuator of the

---

\*BMDP3R was developed at the Health Sciences Computing Facility, UCLA, sponsored by NIH Special Research Resources Grant RR-3. BMDP3R was revised February 16, 1973.

Table 3. Estimated values of the regression constants as a function of frequency for the proposed canopy model of  $\frac{\Delta\sigma^o}{\sigma^o}$  where

$$\frac{\Delta\sigma^o}{\sigma^o} = A \cdot \exp(B \cdot m_s - C \cdot m_p^{1/2} \cdot h^{2.6}) + D \cdot m_p^{1/2} \cdot h$$

Frequency (GHz)	A	B	C	D
8.6	0.469	9.941	- 8.54	0.035
9.4	0.252	11.324	-10.12	0.033
10.2	0.235	14.008	-13.60	0.043
11.0	0.204	14.254	-14.86	0.043
11.8	0.375	13.005	-16.76	0.048
13.0	0.269	12.827	-14.55	0.046
13.8	0.201	13.115	-14.23	0.048
14.6	0.579	8.370	-12.01	0.049
15.4	0.915	6.479	-10.12	0.052
16.2	0.615	5.930	-10.12	0.041
17.0	0.556	6.585	-11.07	0.047

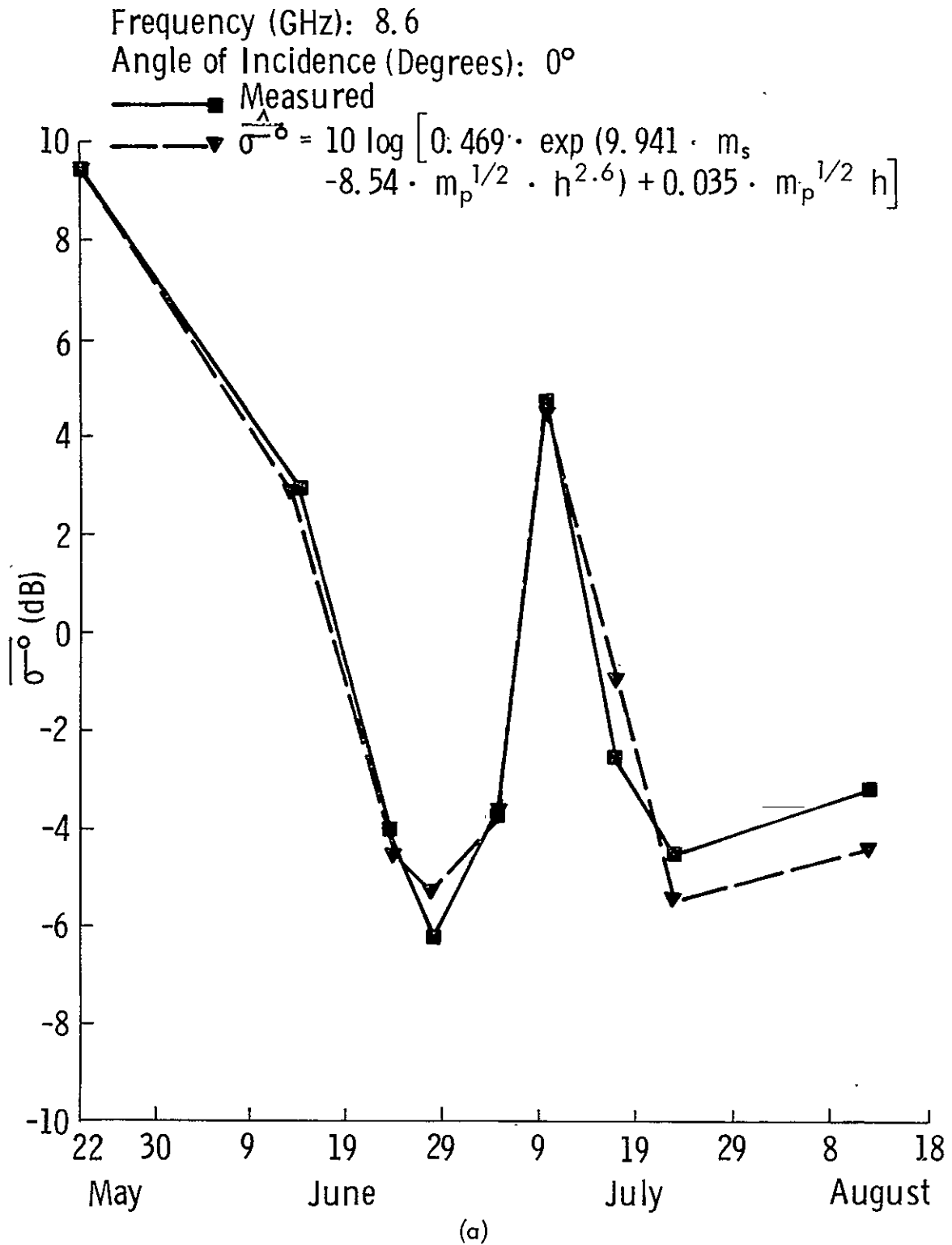
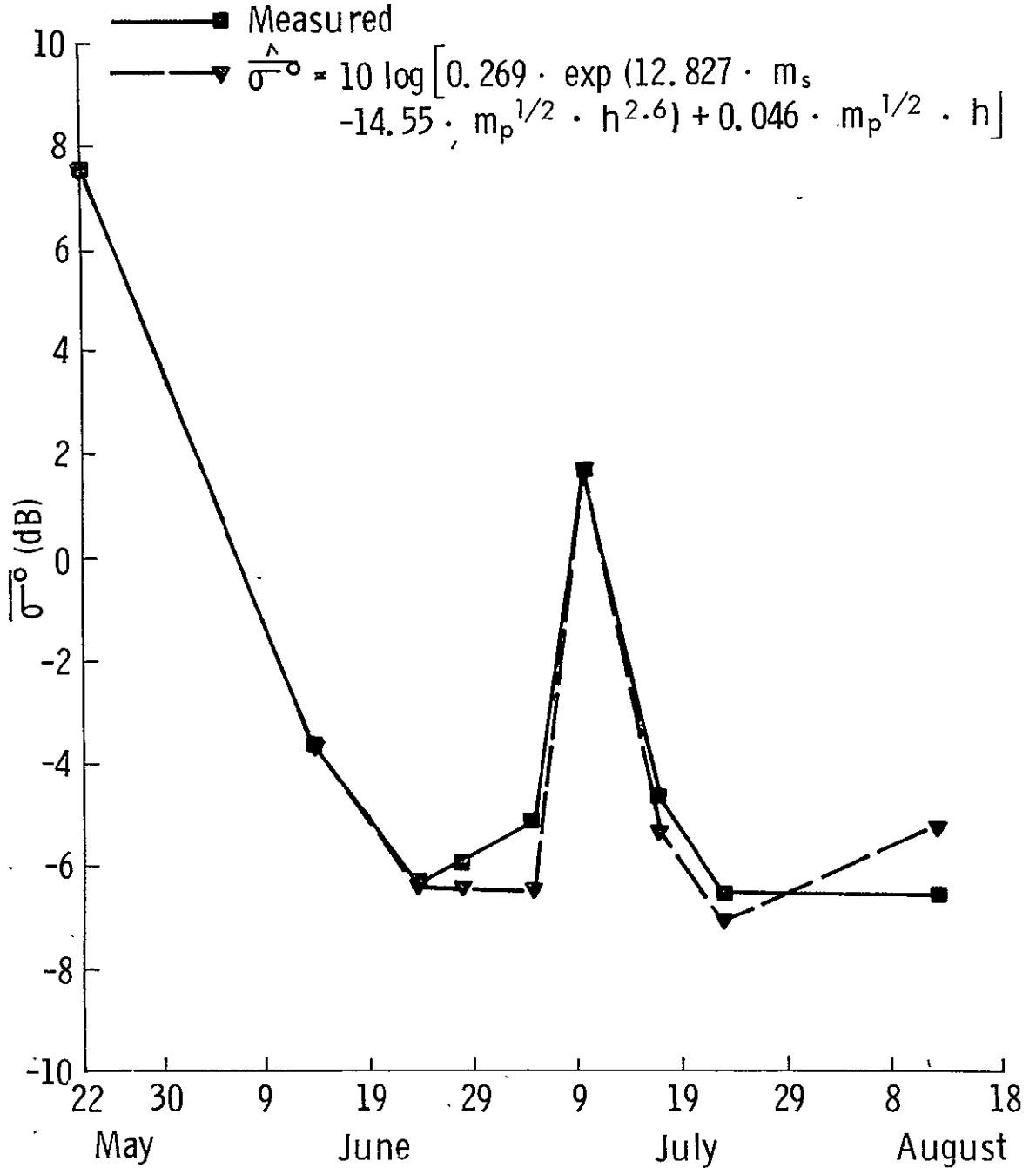


Figure 6. Temporal variations of  $\bar{\sigma}^{\circ}$  (the average value of  $\bar{\sigma}_H^{\circ}$  and  $\bar{\sigma}_V^{\circ}$ ) as measured at nadir with  $\hat{\sigma}^{\circ}$ , the values predicted by the canopy model presented in section 4.0. Data are presented at a) 8.6 GHz, b) 13.0 GHz, and c) 17.0 GHz.

Frequency (GHz): 13.0  
 Angle of Incidence (Degrees): 0°



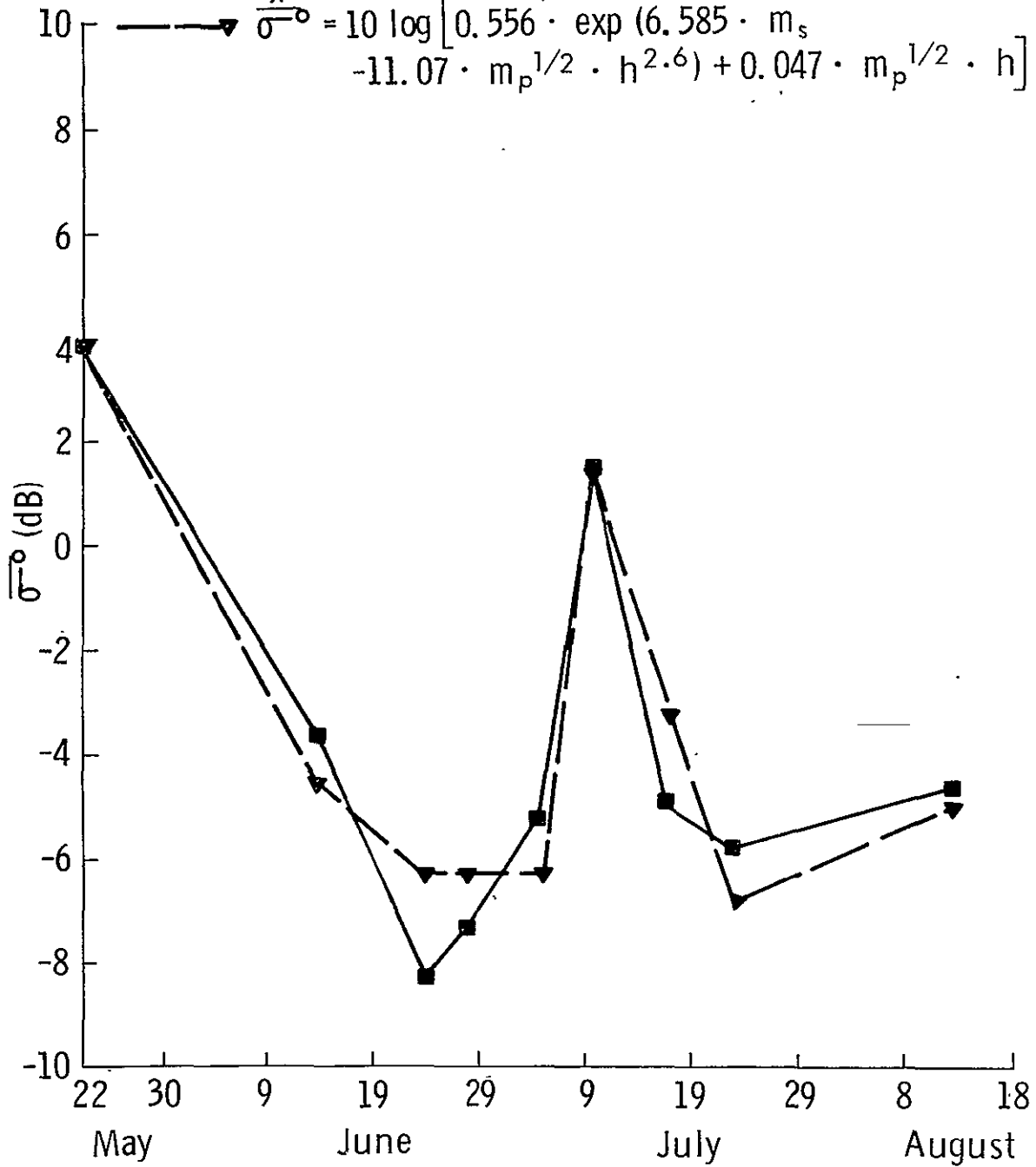
(b)

Frequency (GHz): 17.0

Angle of Incidence: 0°

Measured

$$\hat{\sigma}^{\circ} = 10 \log \left[ 0.556 \cdot \exp(6.585 \cdot m_s) - 11.07 \cdot m_p^{1/2} \cdot h^{2.6} + 0.047 \cdot m_p^{1/2} \cdot h \right]$$



(c)

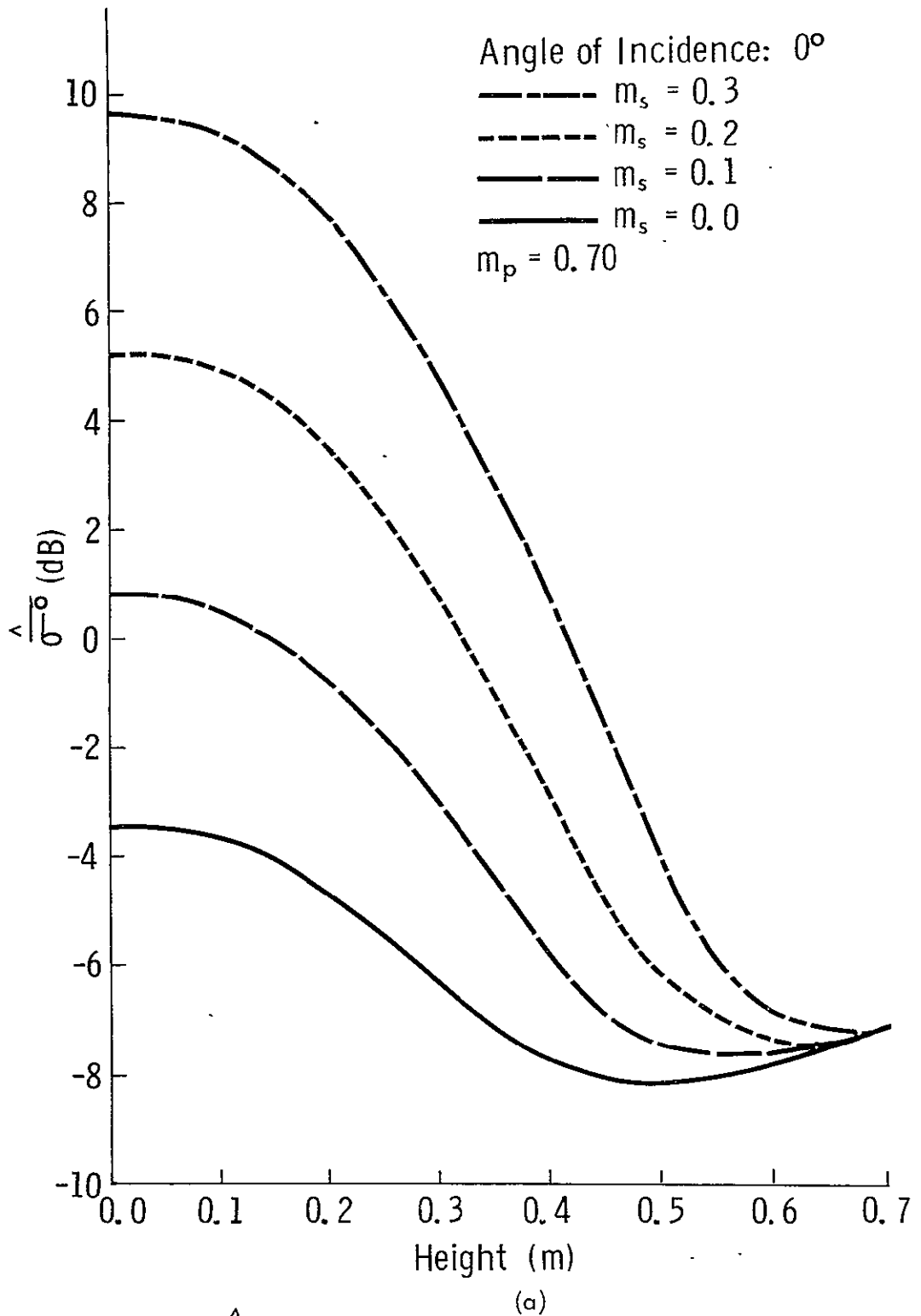
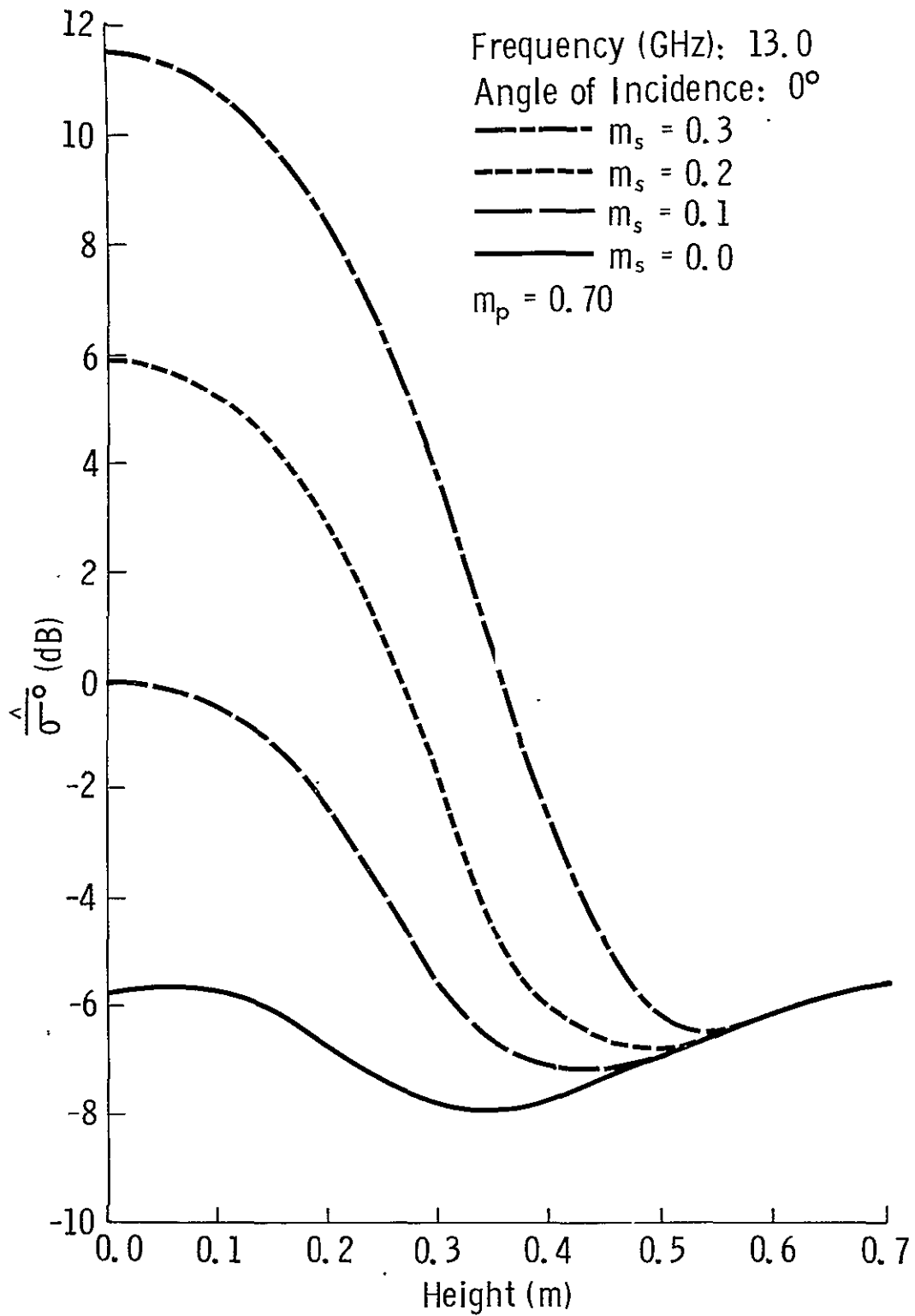
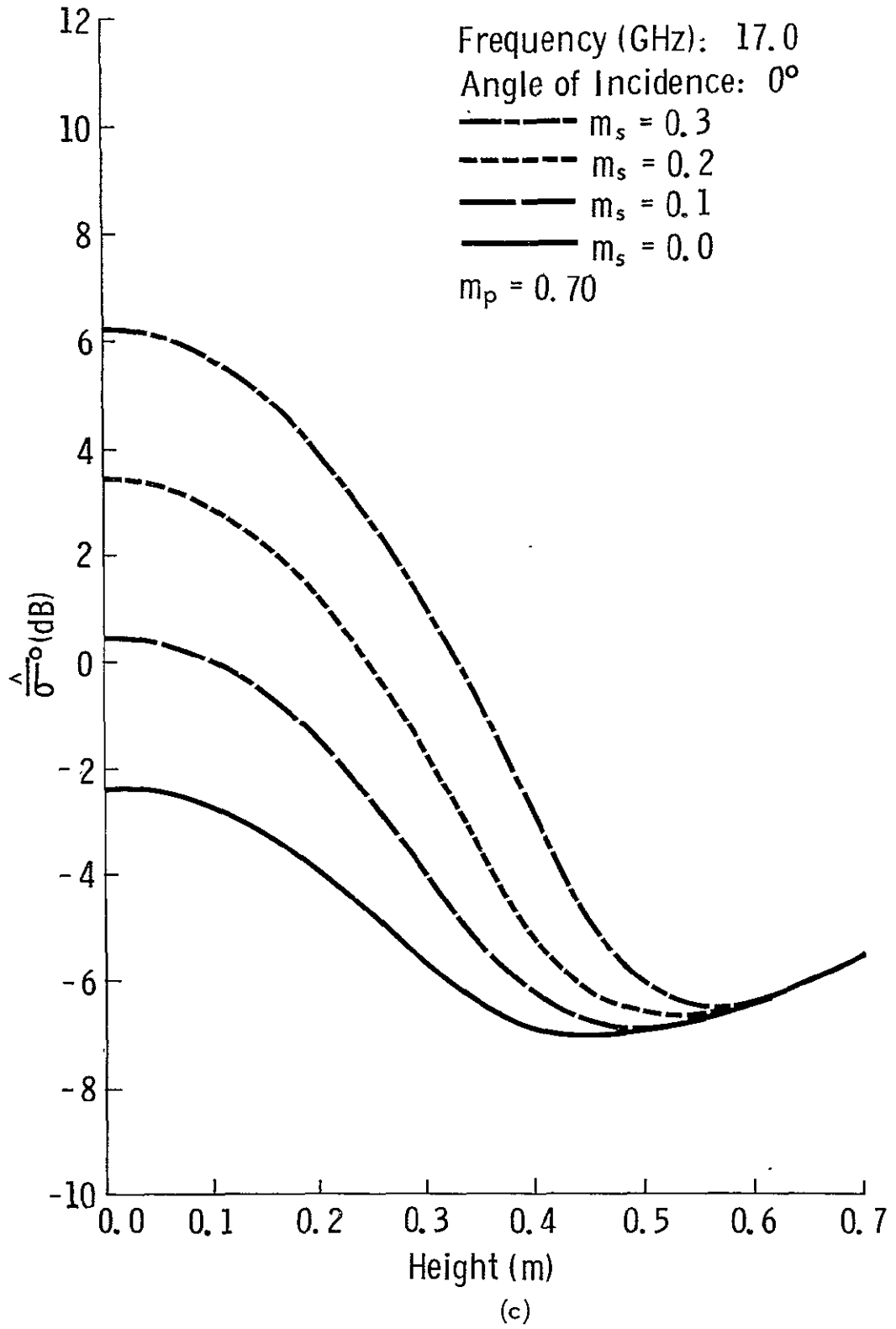


Figure 7. Response of  $\hat{\sigma}^0$ , the value of  $\bar{\sigma}^0$  predicted by the canopy model, as a function of canopy height and soil moisture,  $m_s$ . Curves are presented at a) 8.6 GHz, b) 13.0 GHz, and c) 17.0 GHz.



(b)





soil backscatter component; in other words, the canopy backscatter contribution to the total return is negligible ( $\sigma_c^o \ll \sigma_{cs}^o$  in Equation 14). For  $h > 0.5$  m, on the other hand, the canopy backscatter contribution  $\sigma_c^o$  becomes dominant over  $\sigma_{cs}^o$ . At higher values of  $m_s$ , the position of the minimum in the  $\sigma^o$  versus  $h$  curve increases towards higher values of  $h$ . At  $m_s = 0.3$  g/cm<sup>3</sup>, for example, the minimum is barely discernible at  $h = 0.67$  m.

Figures 7b and 7c present the response of  $\Delta\sigma^o$  to height and soil moisture variations at 13.0 and 17.0 GHz. The effects of the frequency increase are clearly identifiable in these figures. Note that whereas  $\Delta\sigma^o$  showed a dependence on  $m_s$  at a height of 0.5 meters at 8.6 GHz, very little dependence is noted at 13.0 GHz (Figure 7b) or 17.0 GHz (Figure 7c). In fact it appears that  $\Delta\sigma^o$  is totally independent of  $m_s$  for canopy heights greater than 0.55 meters. Attempts to functionally characterize  $\sigma_H^o$  and  $\sigma_V^o$  at angles other than nadir met with little success. While certain temporal trends can be recognized in the data, there does not appear to be any consistent dependence of  $\sigma^o$  upon the measured target characteristics.

### 5.3 Angular Response of $\sigma^o$

Curves depicting  $\sigma^o$  (dB) as a function of angle of incidence often yielded useful information on the "character" of the scattering surface or volume. For this reason a number of examples of the angular response of  $\sigma^o$  of alfalfa under various conditions are now presented. Figures 8a-f present the angular response of  $\sigma_H^o$  and  $\sigma_V^o$  of alfalfa at three frequencies. Two curves representing  $\sigma^o$  for 17 cm alfalfa and 11 cm alfalfa are shown for each frequency-polarization combination. Consider the 8.6 GHz data, Figures 8a and 8b. From these curves we can immediately make two observations. First, assuming the rather short alfalfa had negligible effect on the total backscatter from the target, we note that the soil underlying the alfalfa appears "relatively smooth". This can be inferred from the 10 dB decrease in  $\sigma^o$  as the incidence angle changes from 0° to 10°. Second we note that with the very low vegetation canopy even a small change in  $m_s$  has a marked influence on  $\sigma^o$ . At 0° a change in  $m_s$  from 0.20 g/cm<sup>3</sup> to 0.28 g/cm<sup>3</sup> causes  $\sigma^o$  to increase by about 5 dB. At 13.0 GHz, Figures 8c and 8d, the curves still suggest that a "relatively smooth" description of the soil surface is in order. Also the effect of soil moisture is still apparent. We can note, however, a slight change in the behavior of the curves depicting  $\sigma_V^o$ , particularly in the 20°-70° region where the curves show a tendency to converge, which was not observed at 8.6 GHz. At 17.0 GHz (Figures 8e and 8f) the shape

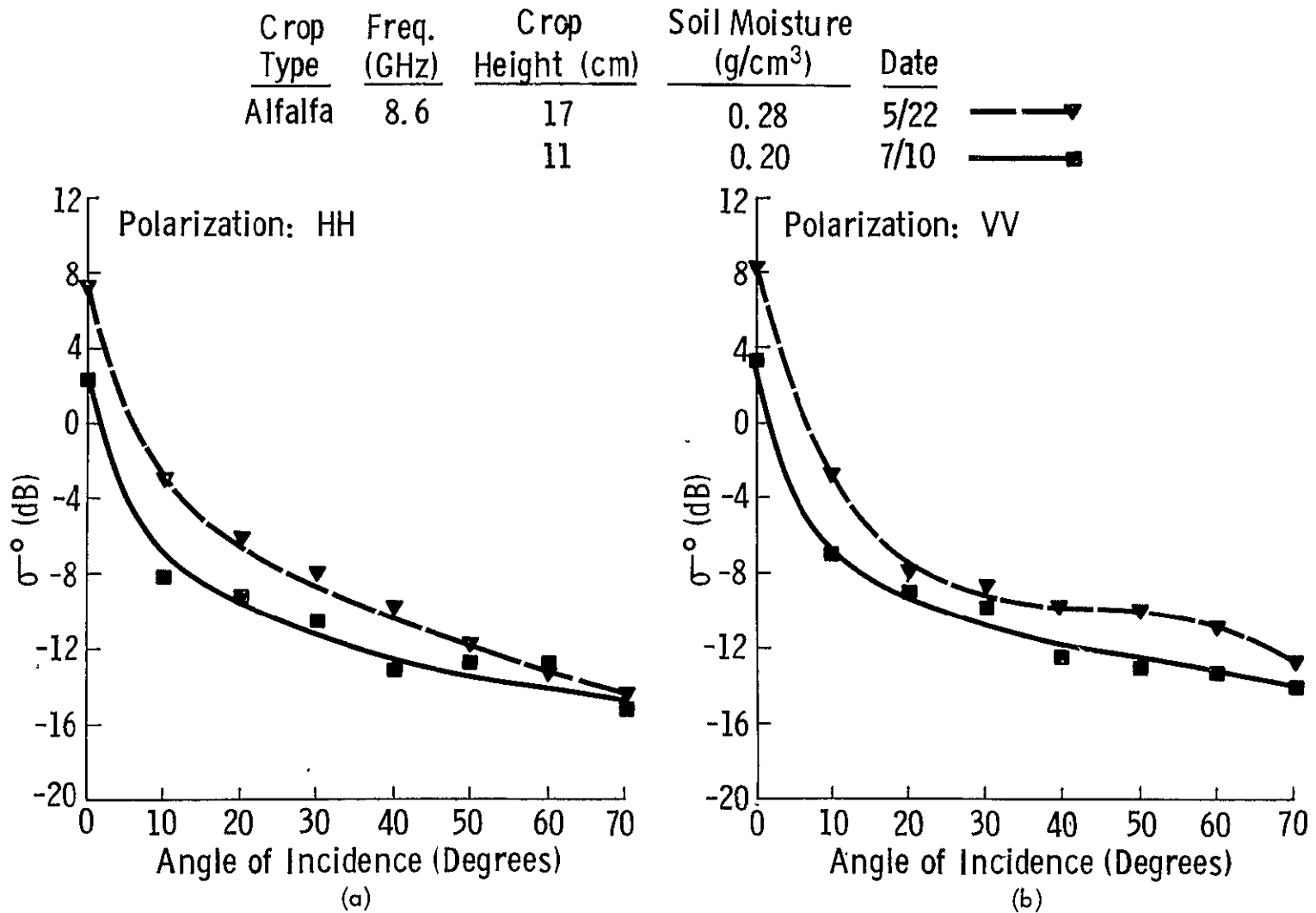
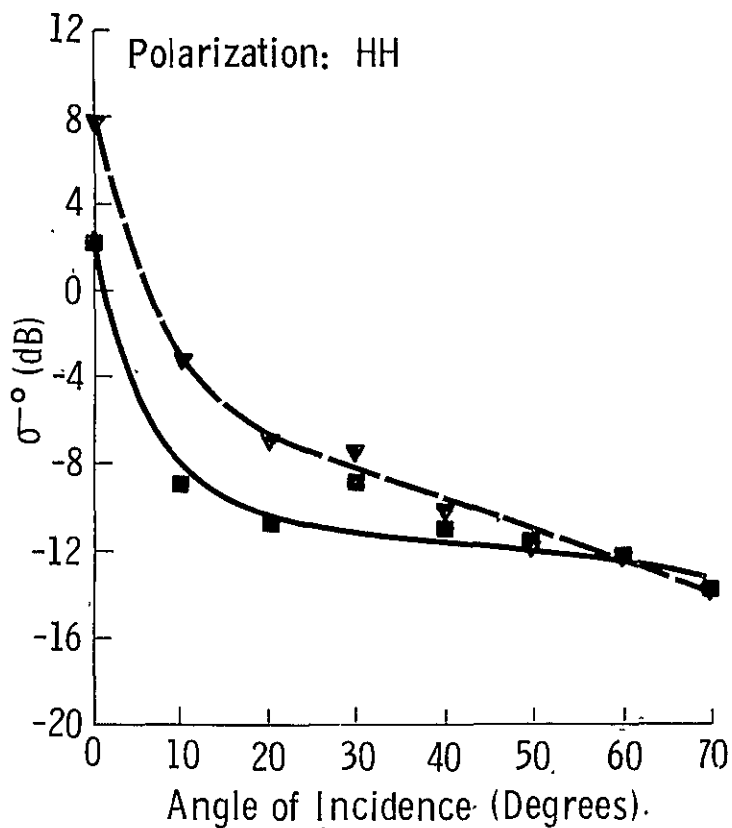


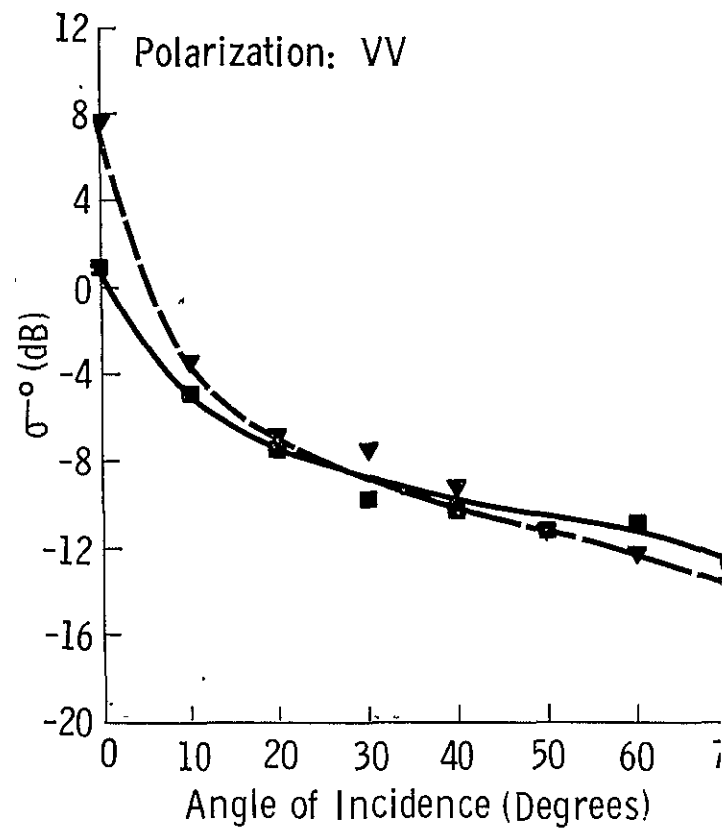
Figure 8. Angular response of  $\sigma^{\circ}$  of harvested alfalfa at 8.6 GHz ( $\sigma_{\text{H}}^{\circ}$  and  $\sigma_{\text{V}}^{\circ}$ , 8a and 8b), 13.0 GHz ( $\sigma_{\text{H}}^{\circ}$  and  $\sigma_{\text{V}}^{\circ}$ , 8c and 8d) and 17.0 GHz ( $\sigma_{\text{H}}^{\circ}$  and  $\sigma_{\text{V}}^{\circ}$ , 8e and 8f). Note that both curves represent  $\sigma^{\circ}$  of harvested alfalfa (11 cm and 17 cm) and that the values of the soil moistures were comparable but not identical.

Crop Type	Freq. (GHz)	Crop Height (cm)	Soil Moisture (g/cm <sup>3</sup> )	Date	Symbol
Alfalfa	13.0	17	0.28	5/22	▼
		11	0.20	7/10	■

30

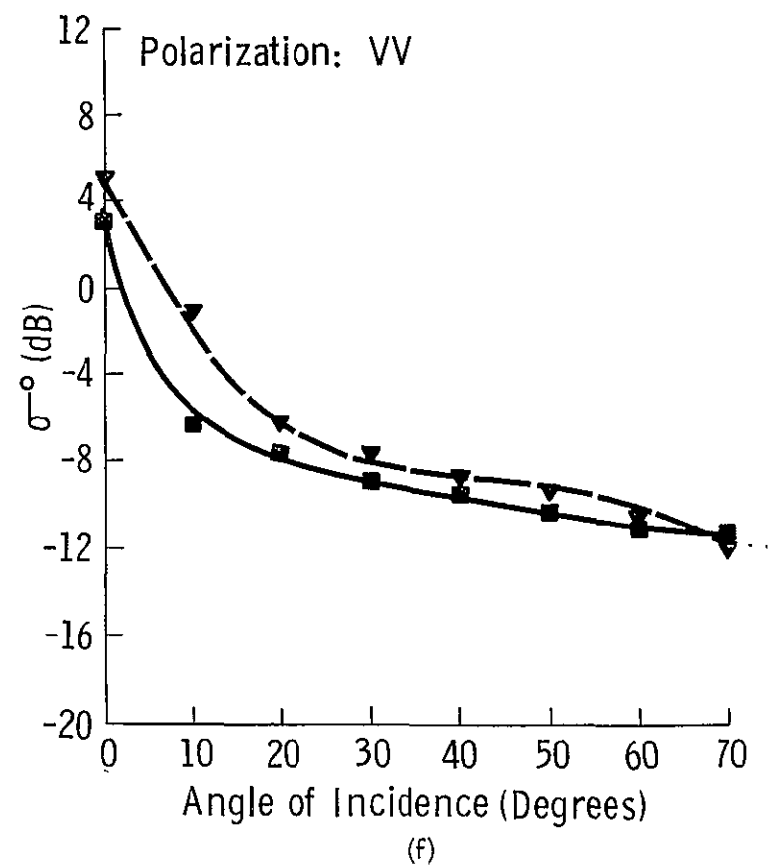
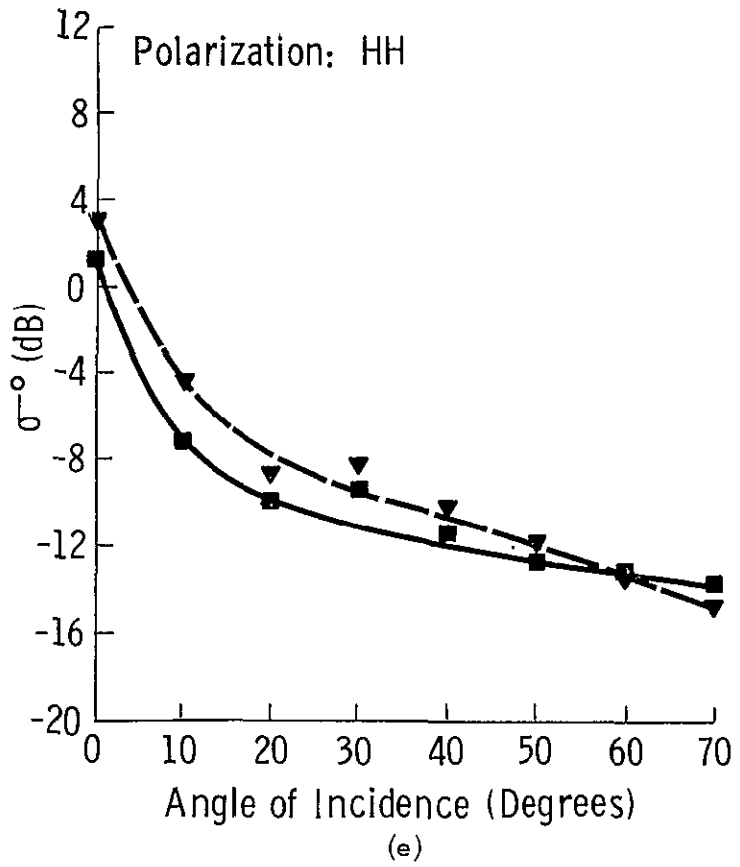


(c)



(d)

Crop Type	Freq. (GHz)	Crop Height (cm)	Soil Moisture (g/cm <sup>3</sup> )	Date	
Alfalfa	17.0	17	0.28	5/22	—▼
		11	0.20	7/10	—■



of the curves in the  $0^\circ$ - $10^\circ$  region begin to imply a slightly rougher surface than noted at the lower frequencies. Now, at 17.0 GHz, we note about an 8 dB or less decrease in  $\sigma^\circ$  from  $0^\circ$  to  $10^\circ$  as contrasted with a 10 dB decrease at 8.6 and 13.0 GHz. Also, it appears that the sensitivity of  $\sigma^\circ$  to variations in soil moisture has been reduced, particularly at nadir.

In Figures 9a-f the angular responses of  $\sigma^\circ$  for two taller stands of alfalfa have been plotted. Note that while the canopies are comparable in height, the soil moistures are markedly different. In Figures 9a and 9b,  $\sigma^\circ$  at 8.6 GHz is presented. While both data sets exhibit nearly identical behavior in the  $10^\circ$ - $70^\circ$  region, the effect of soil moisture is still observed at nadir. An interesting aspect of these curves appears in the  $40^\circ$ - $70^\circ$  region; while  $\sigma_H^\circ$  decreases by about 5 dB from  $40^\circ$  to  $70^\circ$  (Figure 9a),  $\sigma_V^\circ$  decreases by only about 3 dB. Next, consider  $\sigma^\circ$  at 13.0 GHz, Figures 9c and 9d. The effect of soil moisture at nadir is smaller than the effect observed at 8.6 GHz. This is probably the result of added attenuation resulting from the frequency increase. Between  $10^\circ$  and  $70^\circ$ , however, the effect of the frequency increase is merely to increase  $\sigma^\circ$  at all angles without changing the shape of the angular response. At 17.0 GHz, Figures 9e and 9f, this effect of the frequency increase is apparent, particularly for the horizontally polarized data. Also, whereas at 8.6 and 13.0 GHz the curves depicting the two different data sets were usually distinguishable at the higher angles, at 17.0 GHz the curves are very nearly coincident with one another for angles higher than  $20^\circ$ .

Finally consider Figures 10a-f where 17 cm alfalfa is compared to a 55 cm stand of alfalfa. Note that the soil moisture content in both cases are nearly identical. At 8.6 GHz the effect of harvest is again noted to be quite dramatic at nadir. At the higher angles the effect is still apparent although certainly to a much lesser extent. It is interesting to compare the shapes of these two curves as frequency is increased; between 8.6 GHz and 13.0 GHz, for example, a marked change in the shape of the  $\sigma^\circ$  response of the 55 cm canopy is observed, particularly for  $\sigma_V^\circ$ . The shape of this curve indicates that the target assumed a rather rough electromagnetic character while the effect on  $\sigma_V^\circ$  for the 17 cm canopy was relatively minimal. At 17.0 GHz however, both targets assume a rough appearance. While the taller target continued to appear rough the shorter canopy changed remarkably, in terms of roughness, between 13.0 and 17.0 GHz causing the curves to be quite similar in the  $30^\circ$ - $70^\circ$  region. Similar effects are noted for  $\sigma_H^\circ$  although the response to frequency is not nearly so marked as for  $\sigma_V^\circ$ .

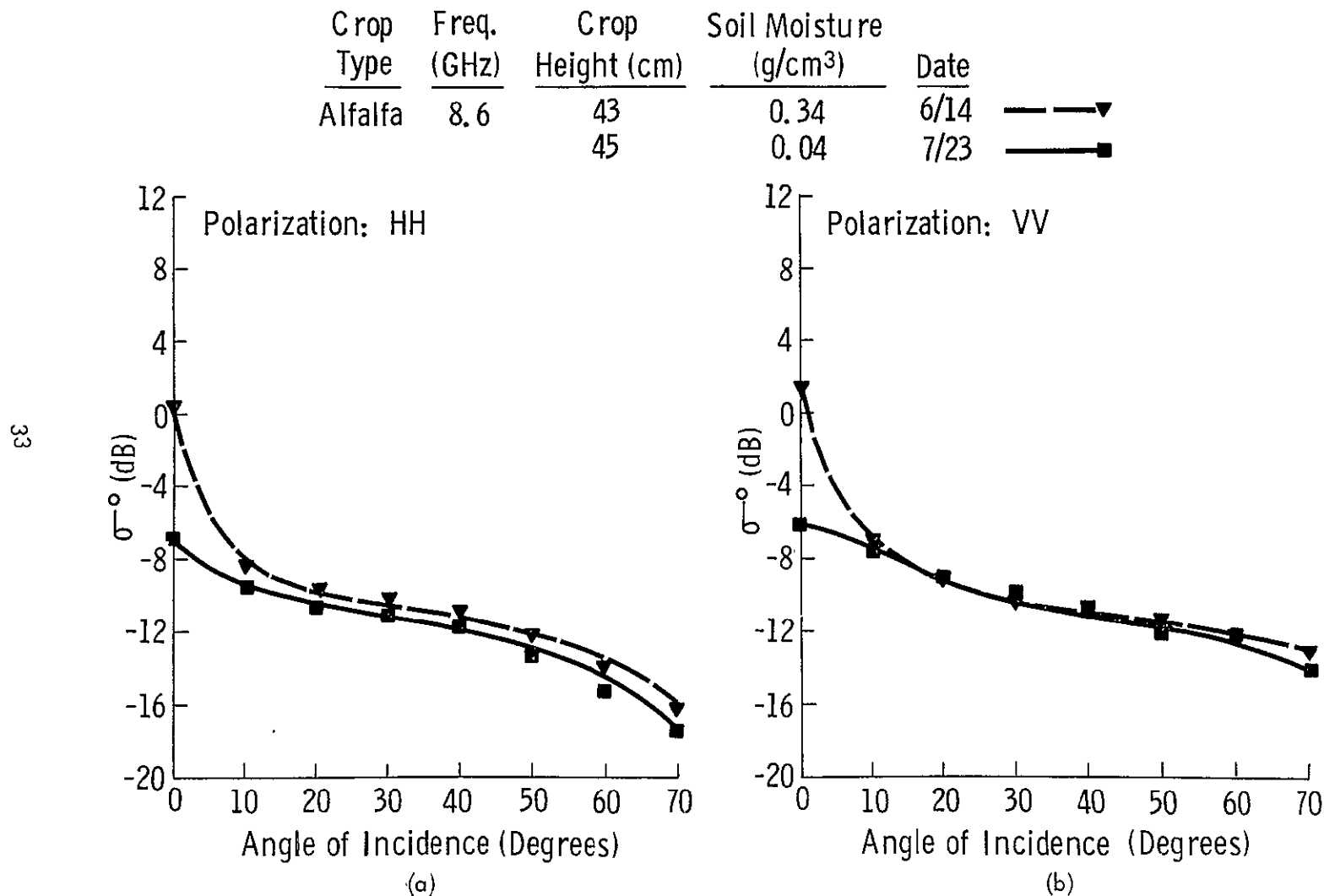
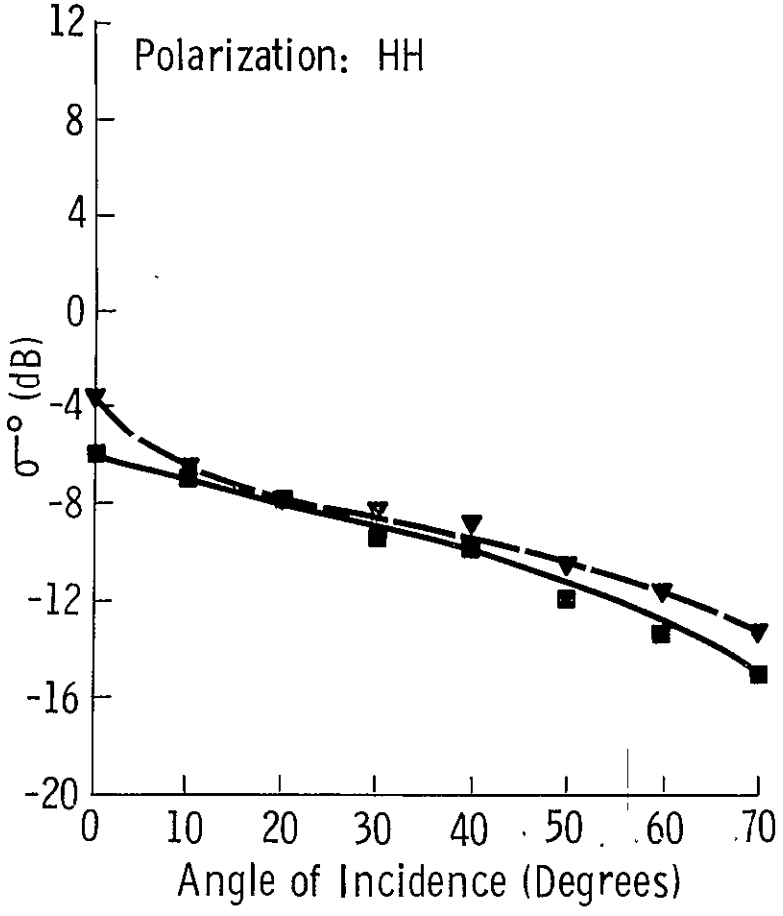
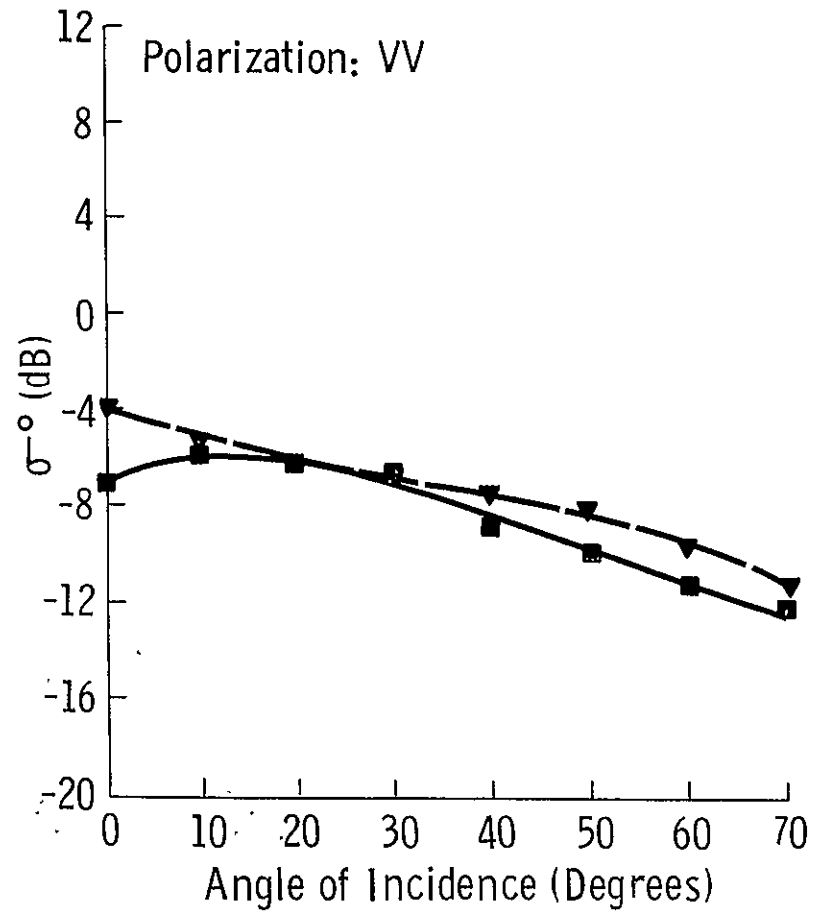


Figure 9. Angular response of  $\sigma^{\circ}$  of two nearly mature stands of alfalfa at 8.6 GHz ( $\sigma_{H}^{\circ}$  and  $\sigma_{V}^{\circ}$ ; 9a and 9b), 13.0 GHz ( $\sigma_{H}^{\circ}$  and  $\sigma_{V}^{\circ}$ , 9c and 9d), and 17.0 GHz ( $\sigma_{H}^{\circ}$  and  $\sigma_{V}^{\circ}$ , 9e and 9f). Although the crop heights are practically identical, the measured values of soil moisture are quite different.

Crop Type	Freq. (GHz)	Crop Height (cm)	Soil Moisture (g/cm <sup>3</sup> )	Date	
Alfalfa	13.0	43	0.34	6/14	—▼
		45	0.04	7/23	—■



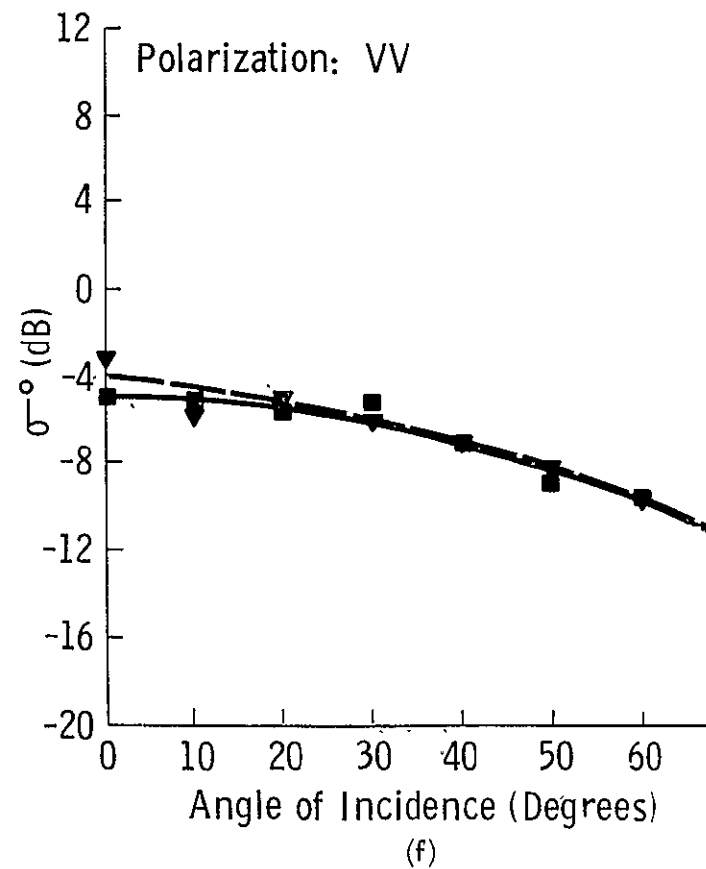
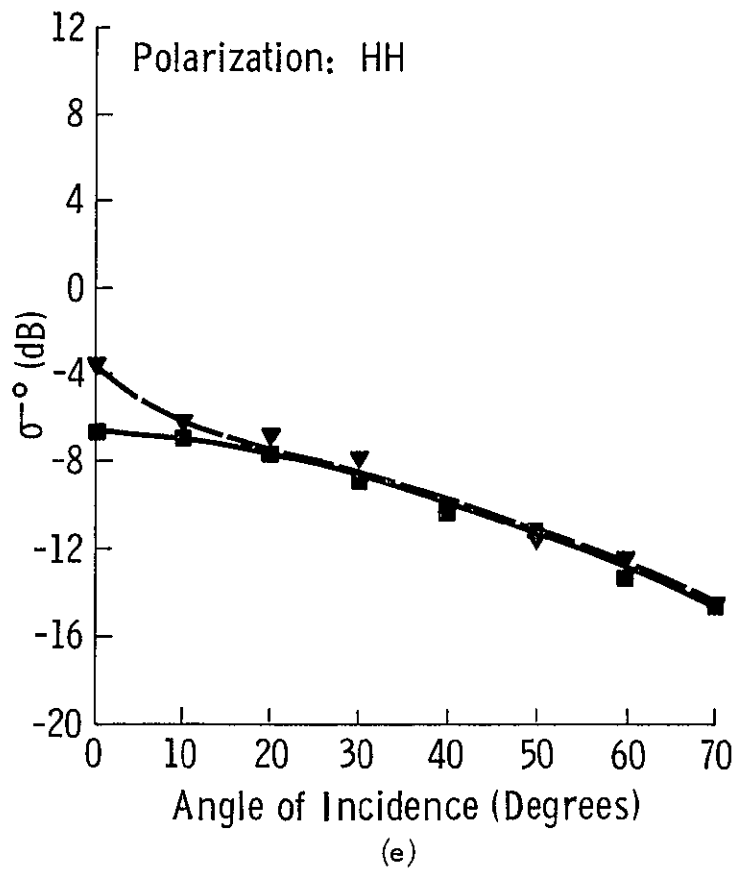
(c)



(d)



Crop Type	Freq. (GHz)	Crop Height (cm)	Soil Moisture (g/cm <sup>3</sup> )	Date	
Alfalfa	17.0	43	0.34	6/14	—▼
		45	0.04	7/23	—■



Crop Type	Freq. (GHz)	Crop Height (cm)	Soil Moisture (g/cm <sup>3</sup> )	Date	
Alfalfa	8.6	17	0.28	5/22	—▲—
		55	0.26	6/24	—■—

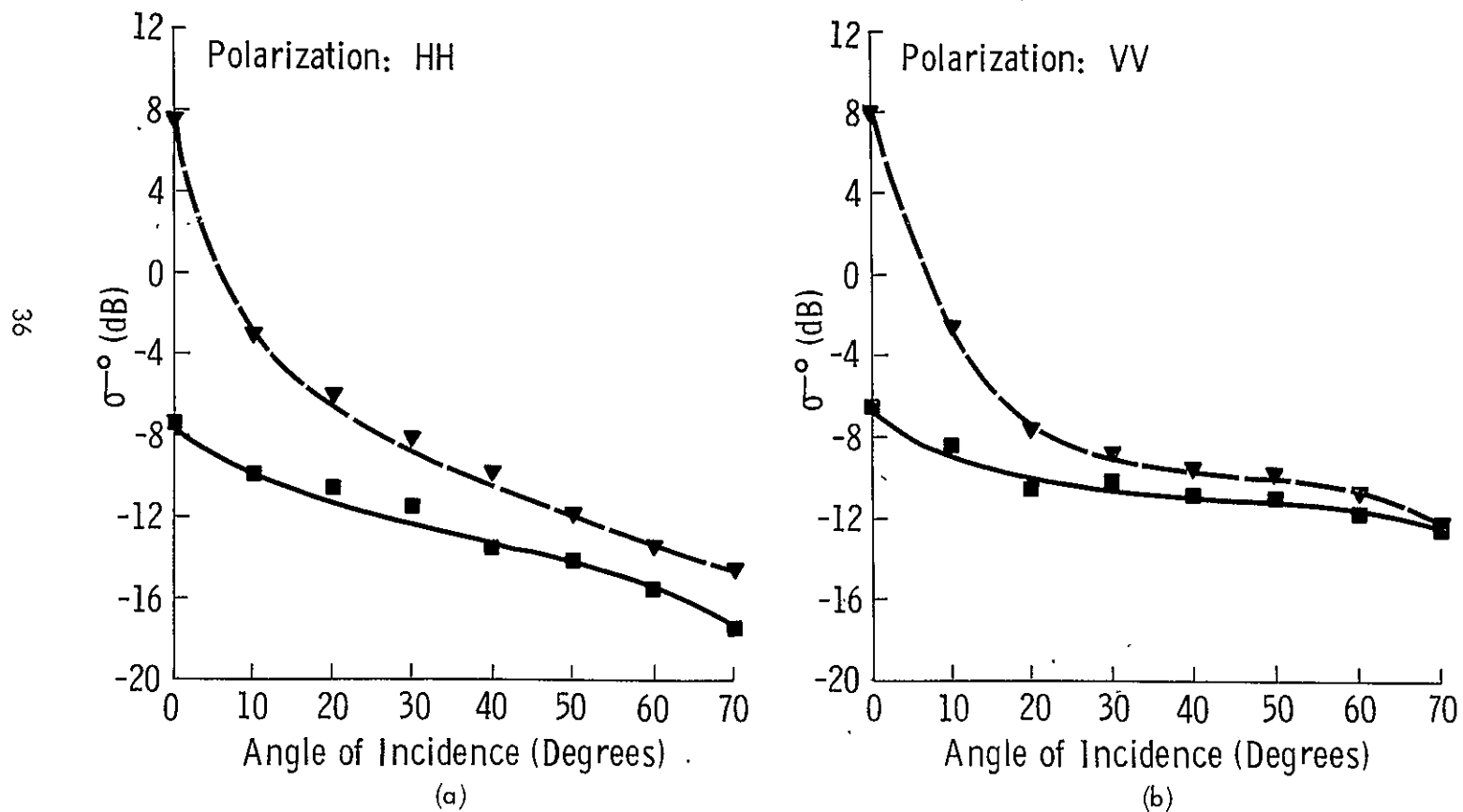
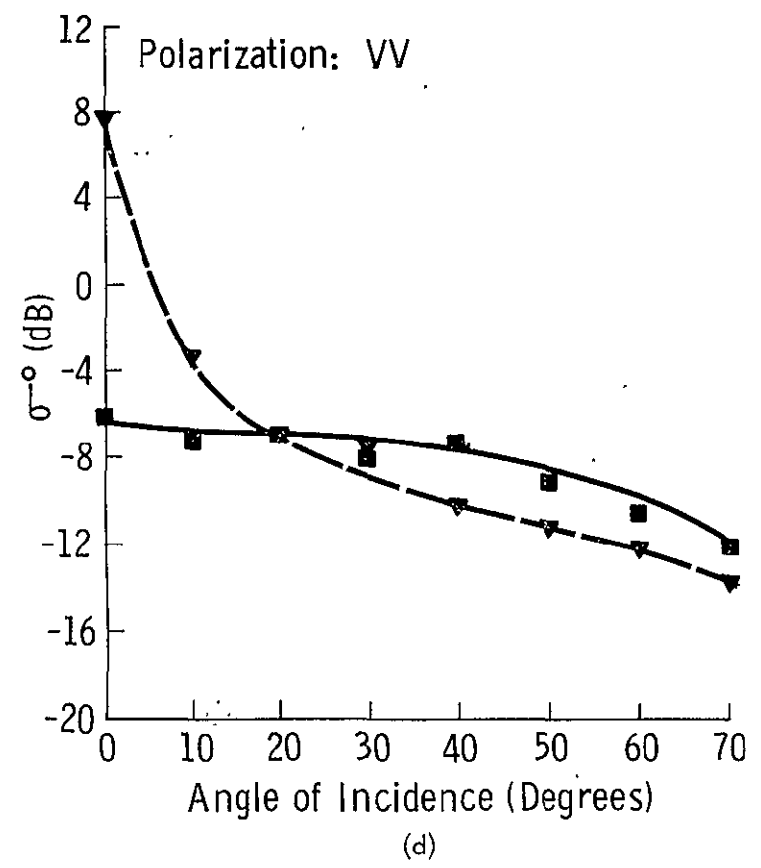
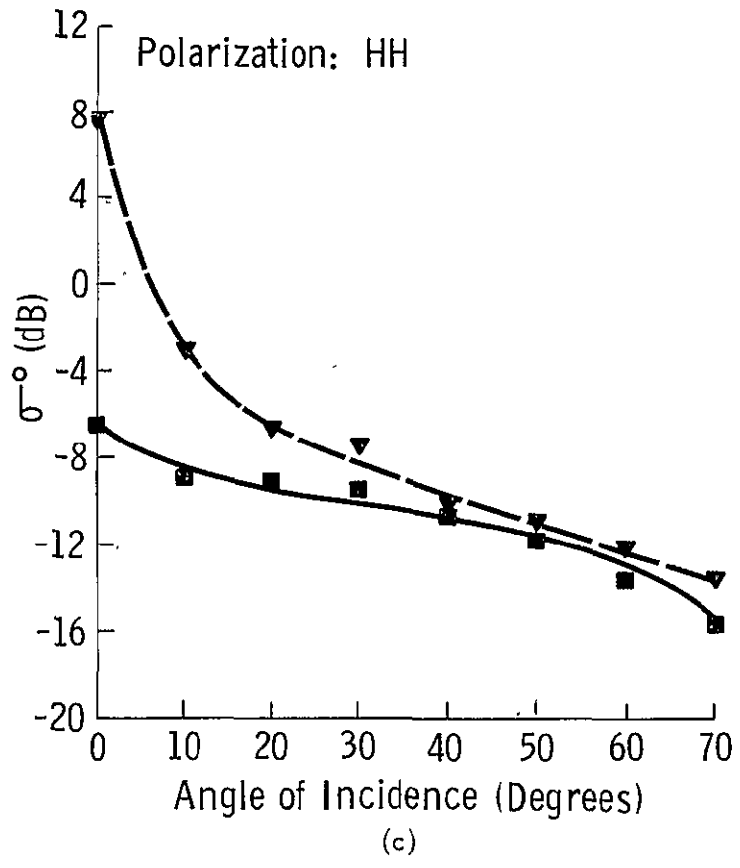


Figure 10. Angular response of  $\sigma^o$  of harvested and mature alfalfa at 8.6 GHz ( $\sigma_{HH}^o$  and  $\sigma_{VV}^o$ , 10a and 10b), 13.0 GHz ( $\sigma_{HH}^o$  and  $\sigma_{VV}^o$ , 10c and 10d), and 17.0 GHz ( $\sigma_{HH}^o$  and  $\sigma_{VV}^o$ , 10e and 10f). Note the soil moistures which are nearly equal.

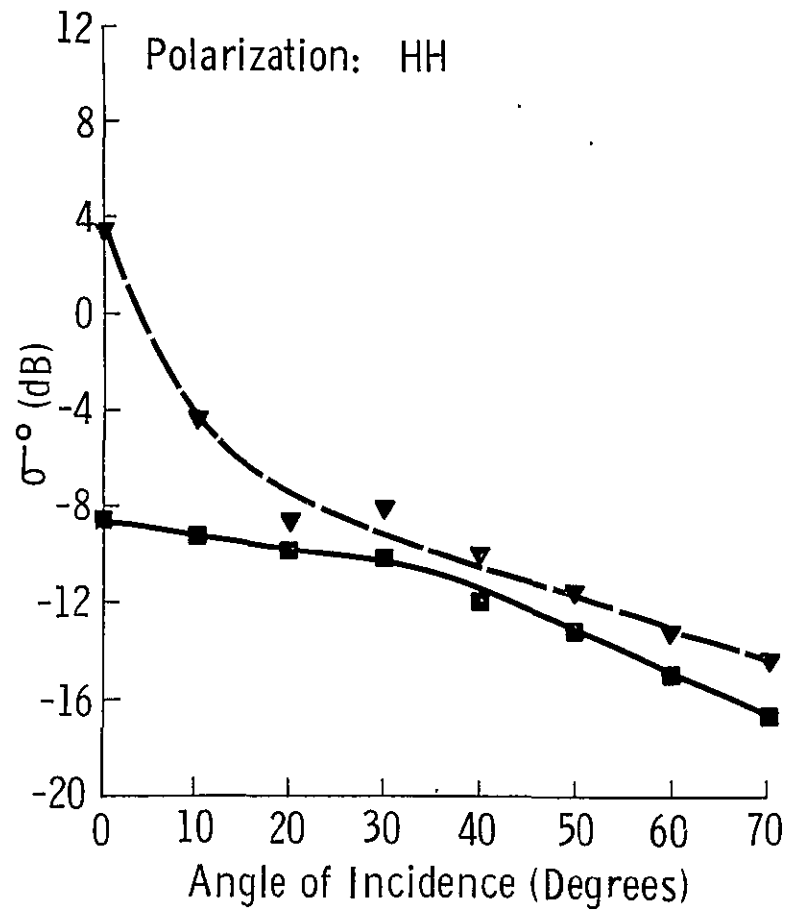
Crop Type	Freq. (GHz)	Crop Height (cm)	Soil Moisture (g/cm <sup>3</sup> )	Date	
Alfalfa	13.0	17	0.28	5/22	—▼
		55	0.26	6/24	—■



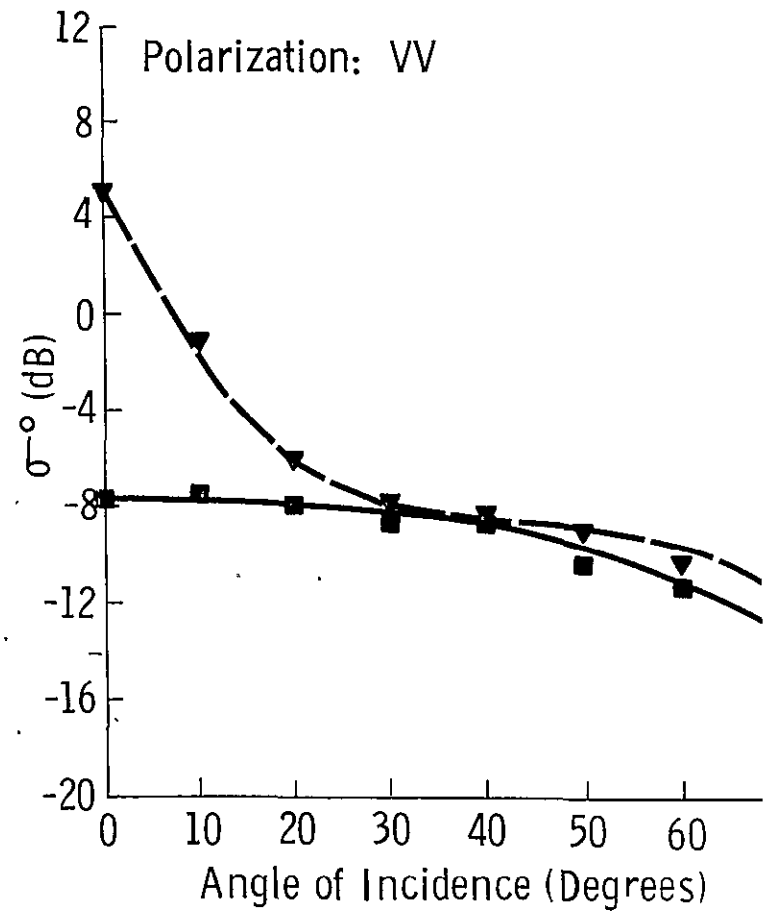
Crop Type	Freq. (GHz)	Crop Height (cm)	Soil Moisture (g/cm <sup>3</sup> )	Date
Alfalfa	17.0	17	0.28	5/22
		55	0.26	6/24

- - - ▾  
 — ■

38



(e)



(f)

#### 5.4 Spectral Response of $\sigma^{\circ}$

In this section two data sets have been chosen for discussion. The first was collected on May 22, 1974 when the alfalfa was 17 cm tall and the soil moisture was  $0.28 \text{ g/cm}^3$ . The second set was collected when the crop had grown to a height of 43 cm with a soil moisture content of  $0.34 \text{ g/cm}^3$ .

Figures 11a and 11b present data collected at nadir. The abscissa presents the frequency in GHz while the ordinate presents  $\sigma^{\circ}$  in dB. While both data sets show a trend for  $\sigma^{\circ}$  to decrease with frequency, Figure 11b, presenting  $\sigma^{\circ}$  for the taller crop, seems to remain rather constant at frequencies above 11.8 GHz. This is not the case for  $\sigma^{\circ}$  representing the shorter stand of alfalfa which may be attributed to differences in roughness. As frequency is increased for the short crop, the underlying soil will become progressively rougher in an electromagnetic sense. This increase in roughness would result in a decrease in the amount of energy backscattered. The taller target, however, will probably look relatively rough even at 8.6 GHz. As frequency increases the taller stand of alfalfa will look rougher until it approaches a Lambertian surface, at which point an increase in frequency will have a rather small effect.

For completeness Figures 11c-h present spectral data at  $30^{\circ}$ ,  $50^{\circ}$  and  $70^{\circ}$ . While these data show a dependency on frequency it is difficult to relate these dependencies to the target characteristics. It should be noted however, that at angles of  $30^{\circ}$ ,  $50^{\circ}$  and  $70^{\circ}$ ,  $\sigma^{\circ}$  for the 43 cm canopy shows an increasing trend while  $\sigma^{\circ}$  for the 17 cm canopy shows relatively little tendency to increase.

#### 6.0 CONCLUDING REMARKS

Experimental measurements of the backscattering coefficient  $\sigma^{\circ}$  of alfalfa in the 8-18 GHz frequency range indicate that at nadir  $\sigma^{\circ}$  responds to variations in plant height and soil moisture content. For tall stands of alfalfa, attenuation by the vegetation masks the effect of soil moisture variations, while for short stands, the majority of the return is contributed by the soil. A semi-empirical semi-theoretical backscatter model was developed for a continuous vegetation canopy in terms of measurable target parameters (plant height, plant moisture content and soil moisture content). Attempts to fit the developed expression to the measured data

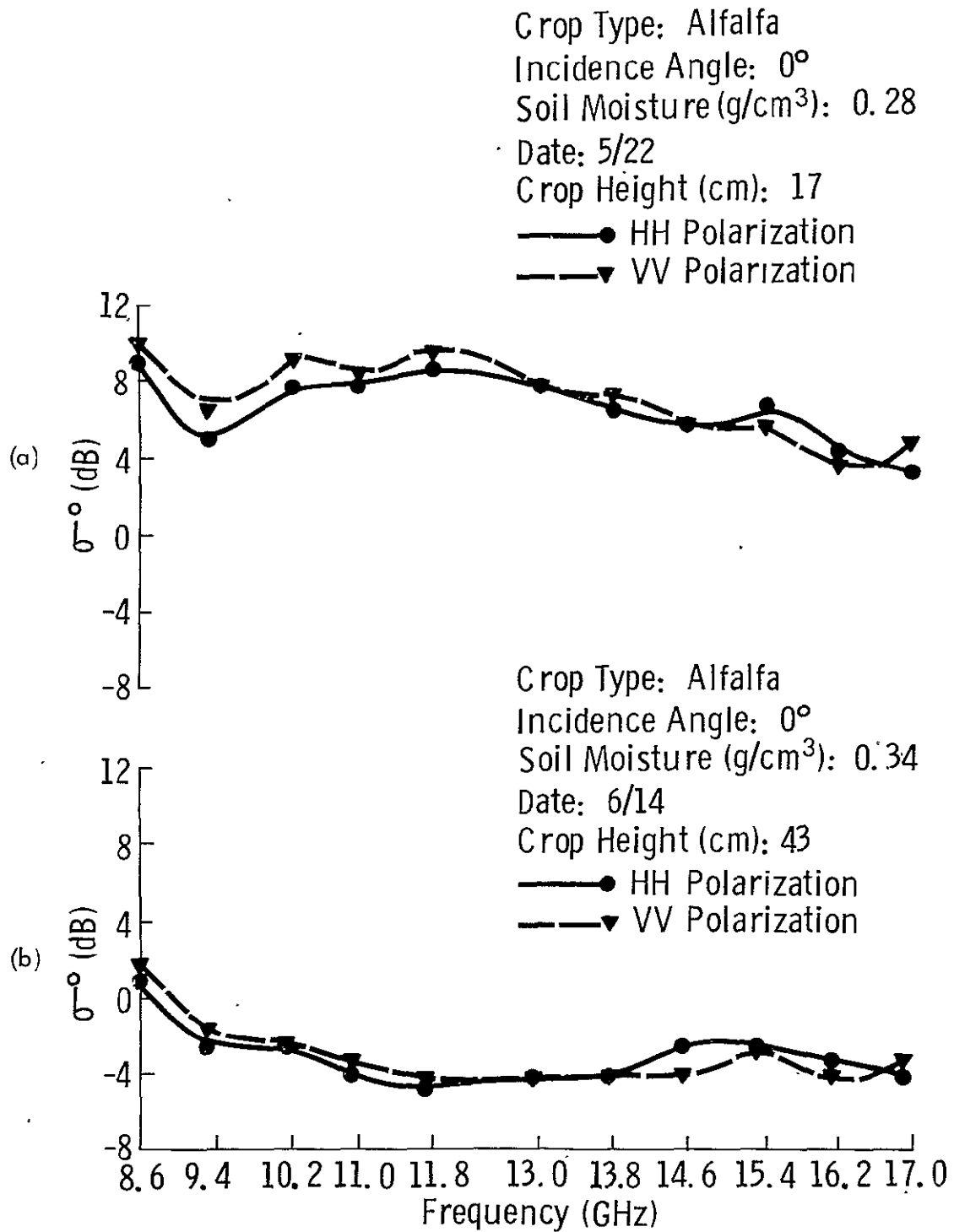
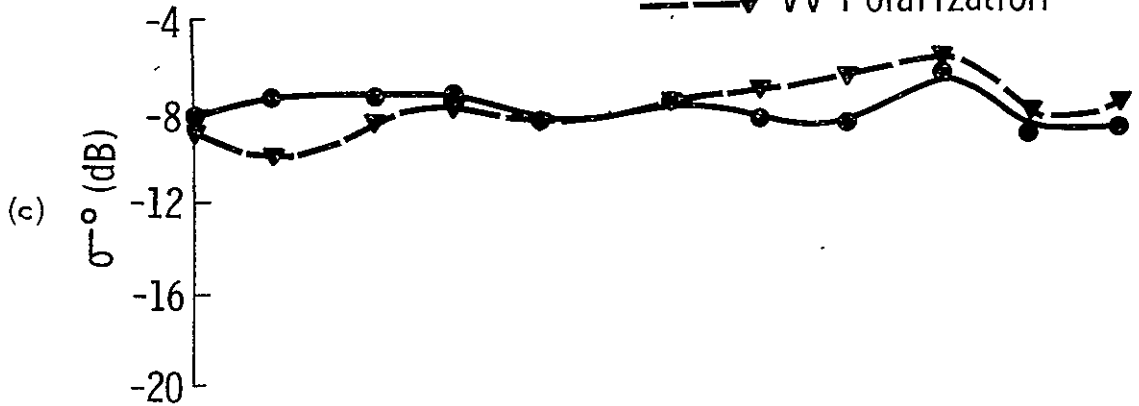
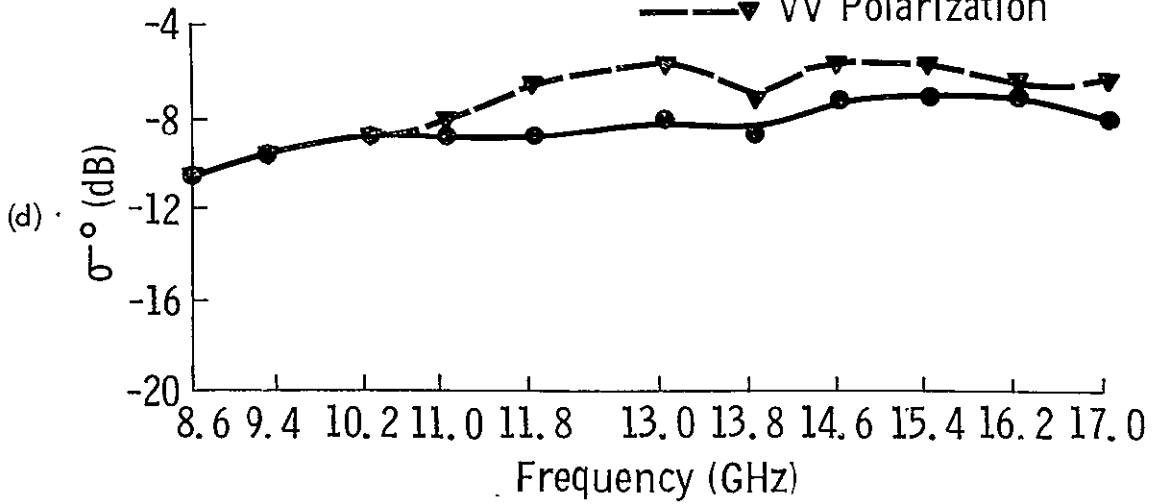


Figure 11. Spectral response of  $\sigma_H^0$  and  $\sigma_V^0$  for two stands of alfalfa at different growth stages at  $0^\circ$  (a and b),  $30^\circ$  (c and d),  $50^\circ$  (e and f), and  $70^\circ$  (g and h).

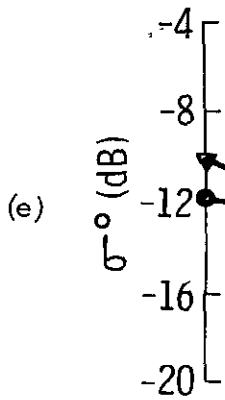
Crop Type: Alfalfa  
 Incidence Angle: 30°  
 Soil Moisture (g/cm<sup>3</sup>): 0.28  
 Date: 5/22  
 Crop Height (cm): 17  
 —●— HH Polarization  
 - - - ▾ VV Polarization



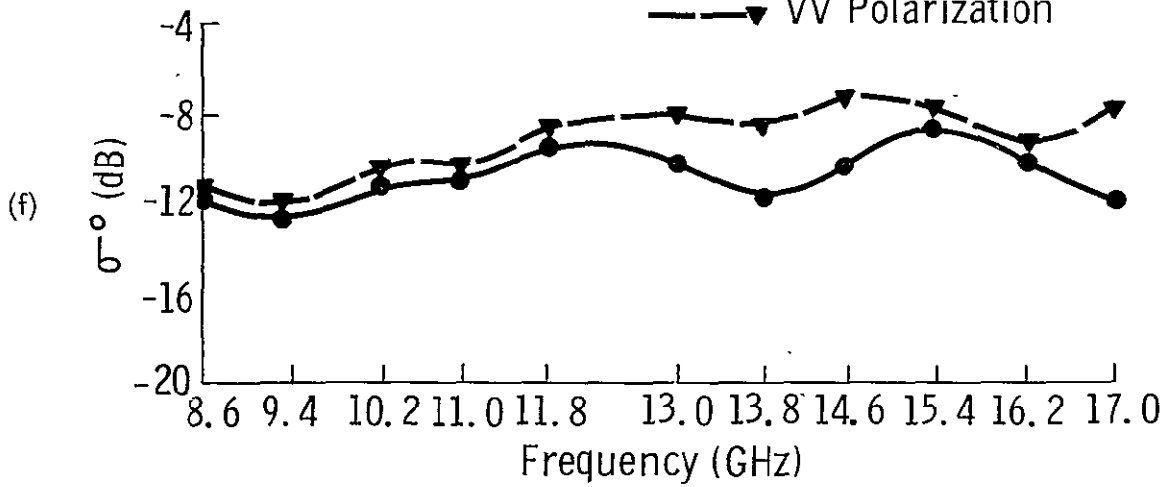
Crop Type: Alfalfa  
 Incidence Angle: 30°  
 Soil Moisture (g/cm<sup>3</sup>): 0.34  
 Date: 6/14  
 Crop Height (cm): 43  
 —●— HH Polarization  
 - - - ▾ VV Polarization



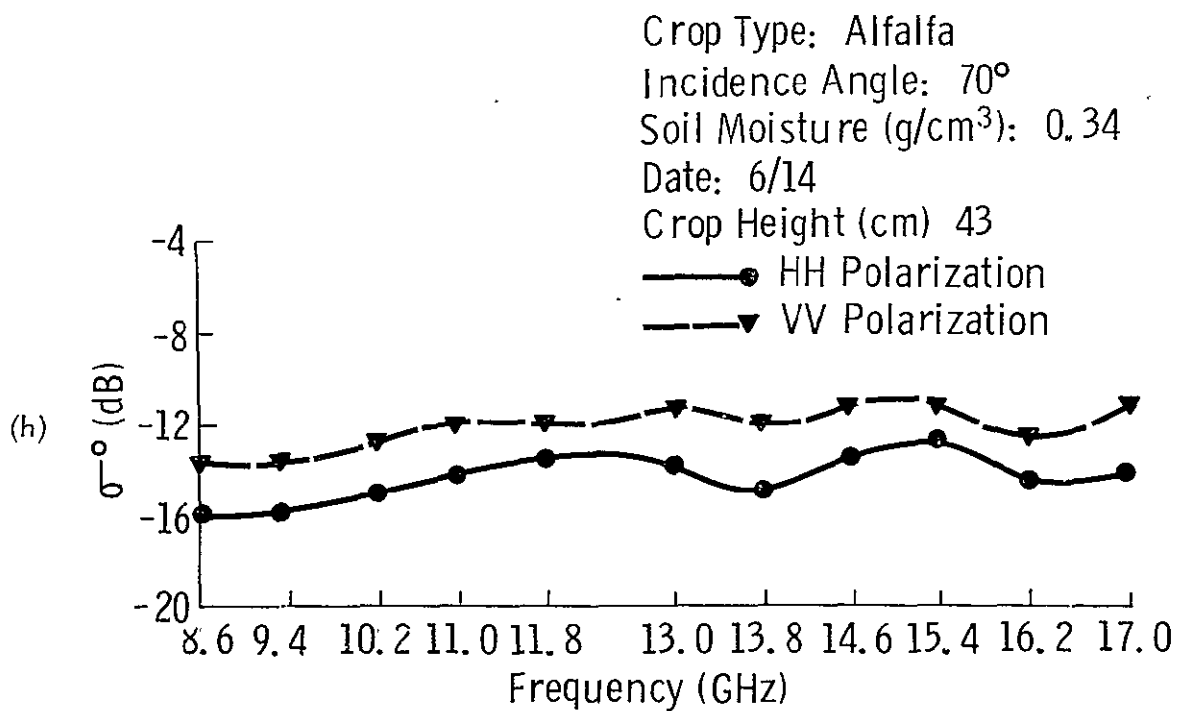
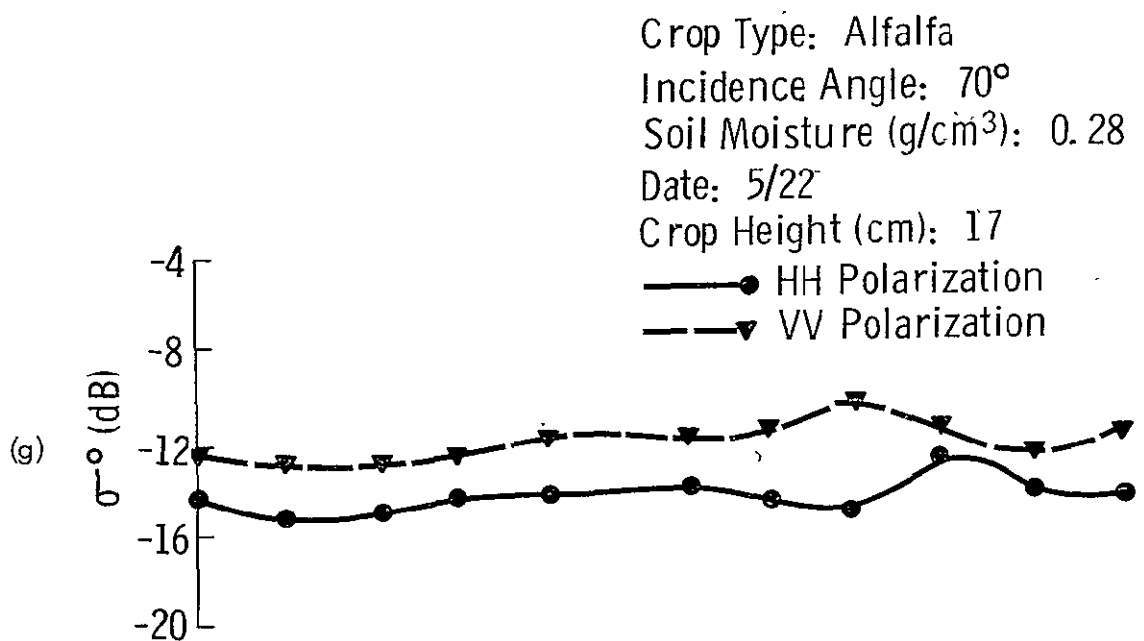
Crop Type: Alfalfa  
 Incidence Angle: 50°  
 Soil Moisture (g/cm<sup>3</sup>): 0.28  
 Date: 5/22  
 Crop Height (cm): 17  
 —●— HH Polarization  
 - - - ▾ VV Polarization



Crop Type: Alfalfa  
 Incidence Angle: 50°  
 Soil Moisture (g/cm<sup>3</sup>): 0.34  
 Date: 6/14  
 Crop Height (cm): 43  
 —●— HH Polarization  
 - - - ▾ VV Polarization







yielded very satisfactory results at nadir. At angles of incidence away from nadir, however, the temporal variations of  $\sigma^{\circ}$  did not show a consistent response to any one of the measurable target parameters.

The promising aspect of this study and others [10, 11] is that the response of  $\sigma^{\circ}$ , near nadir, to variations in the height of alfalfa appears to be rather consistent. It is this sort of consistency that is needed for studying the various agricultural targets of interest on an operational basis.

## REFERENCES

- [1] Bush, T. F. and F. T. Ulaby, "8-18 GHz Radar Spectrometer," RSL Technical Report 177-43, University of Kansas Center for Research, Inc., Lawrence, Kansas, September, 1973.
- [2] Bush, T. F. and F. T. Ulaby, "Fading Characteristics of Panchromatic Radar Backscatter from Selected Agricultural Targets," IEEE Transactions on Geoscience Electronics, vol. GE-14, October, 1975.
- [3] Cihlar, J., "Ground Data Acquisition Procedure for Microwave (MAPS) Measurements," RSL Technical Memorandum 177-42, University of Kansas Center for Research, Inc., Lawrence, Kansas, July, 1973.
- [4] Cihlar, J. and F. T. Ulaby, "Dielectric Properties of Soils as a Function of Moisture Content," RSL Technical Report 177-47, University of Kansas Center for Research, Inc., Lawrence, Kansas, November, 1974.
- [5] Carlson, N. L., "Dielectric Constant of Vegetation at 8.5 GHz," Ohio State University, Electro Science Lab., Tech. Report 1903-5, 1967.
- [6] Ulaby, F. T., J. Cihlar and R. K. Moore, "Active Microwave Measurement of Soil Water Content," Remote Sensing of Environment, vol. 3, pp. 185-203, January, 1974.
- [7] Lane, J. A. and J. A. Saxton, "Dielectric Dispersion in Pure Polar Liquids at Very High Radio-Frequencies. I. Measurements on Water, Methyl and Ethyl Alcohols," Proc. Roy. Soc. London, vol. 214, pp. 531-545, 1951.
- [8] Peake, William H., "Interaction of Electromagnetic Waves with Some Natural Surfaces," IRE Trans. on Antennas and Propagation, pp. S324-S329, December, 1959.
- [9] Ulaby, F. T., "Radar Response to Vegetation," IEEE Transactions on Antennas and Propagation, vol. AP-23, no. 1, January, 1975.
- [10] de Loor, G. P., "Measurement of Radar Ground Returns," Proc. URSI Specialist Meeting on Emission and Scattering from the Earth, Bern, Switzerland, September, 1974.
- [11] Cosgriff, R. L., W. H. Peake and R. C. Taylor, "Terrain Scattering Properties of Sensor System Design," Terrain Handbook II, Engr. Expt. Sta., Ohio State University Bull. 181, May, 1960.

APPENDIX A: Ground Truth Summary for 1974 Alfalfa  
Scattering Experiment

Alfalfa Ground Truth 1974

Date	Soil Moisture (g/cm <sup>3</sup> )			Fractional Plant Moisture	Plant Height (cm)
	N	M	F		
May 22	0.27	0.28	0.28	0.68	17
June 14	0.36	0.34	0.33	0.85	43
June 24	0.26	0.26	0.23	0.78	55
June 28	0.15	0.20	0.17	0.79	55
July 5	0.32	0.30	0.30	0.76	55
July 10	0.14	0.20	0.15	0.60	11
July 17	0.05	0.02	0.02	0.79	29
July 23	0.03	0.04	0.03	0.80	45
August 13	0.21	0.14	0.16	0.77	73

N = near range sample

M = medium range sample

F = far range sample

APPENDIX B: Alfalfa Scattering Coefficients, 1974.

## ANTENNA ANGLE 0

FREQ	8.6	9.4	10.2	11.0	11.8	13.0	13.8	14.6	15.4	16.2	17.0
POL HH	7.1	5.3	7.9	7.6	8.6	7.7	6.5	5.8	6.4	4.1	3.1
POL VV	7.7	6.9	9.2	8.6	9.5	7.7	7.1	6.4	5.7	3.3	4.5

## ANTENNA ANGLE 10

FREQ	8.6	9.4	10.2	11.0	11.8	13.0	13.8	14.6	15.4	16.2	17.0
POL HH	-3.1	-5.3	-3.8	-4.3	-1.0	-3.4	-4.4	-2.8	-1.5	-3.4	-4.4
POL VV	-2.8	-3.3	-2.8	-2.7	-1.2	-3.3	-3.0	-3.5	-1.9	-3.9	-1.4

## ANTENNA ANGLE 20

FREQ	8.6	9.4	10.2	11.0	11.8	13.0	13.8	14.6	15.4	16.2	17.0
POL HH	-6.1	-6.8	-6.1	-5.6	-4.2	-6.9	-6.6	-5.3	-5.2	-8.1	-8.6
POL VV	-7.9	-7.5	-6.1	-5.9	-3.8	-5.6	-5.1	-5.6	-5.4	-6.6	-6.3

## ANTENNA ANGLE 30

FREQ	8.6	9.4	10.2	11.0	11.8	13.0	13.8	14.6	15.4	16.2	17.0
POL HH	-8.1	-7.7	-7.6	-7.4	-8.4	-7.5	-8.1	-8.3	-6.4	-8.8	-8.3
POL VV	-8.8	-10.0	-8.2	-8.0	-8.4	-7.5	-7.0	-6.2	-5.7	-8.5	-7.8

## ANTENNA ANGLE 40

FREQ	8.6	9.4	10.2	11.0	11.8	13.0	13.8	14.6	15.4	16.2	17.0
POL HH	-9.9	-9.8	-9.6	-9.7	-9.2	-10.3	-8.3	-9.1	-8.3	-9.9	-10.2
POL VV	-9.7	-9.8	-8.5	-8.6	-8.4	-8.6	-8.5	-7.5	-7.6	-9.1	-8.5

## ANTENNA ANGLE 50

FREQ	8.6	9.4	10.2	11.0	11.8	13.0	13.8	14.6	15.4	16.2	17.0
POL HH	-11.9	-12.1	-11.7	-11.3	-11.3	-11.0	-11.1	-9.8	-8.8	-11.2	-11.7
POL VV	-10.0	-11.2	-13.8	-10.4	-9.9	-9.9	-10.1	-7.8	-8.8	-13.5	-9.4

## ANTENNA ANGLE 60

FREQ	8.6	9.4	10.2	11.0	11.8	13.0	13.8	14.6	15.4	16.2	17.0
POL HH	-13.4	-13.5	-13.1	-12.4	-12.7	-12.3	-13.1	-12.0	-11.1	-12.6	-13.4
POL VV	-11.0	-11.7	-11.0	-10.9	-9.8	-10.7	-10.6	-9.6	-10.1	-11.2	-10.4

## ANTENNA ANGLE 70

FREQ	8.6	9.4	10.2	11.0	11.8	13.0	13.8	14.6	15.4	16.2	17.0
POL HH	-14.5	-15.2	-14.8	-14.2	-14.0	-13.7	-14.4	-13.3	-12.9	-14.4	-14.5
POL VV	-12.6	-12.9	-12.3	-12.2	-11.5	-11.5	-11.4	-10.6	-11.1	-12.6	-11.7

## ANTENNA ANGLE 0

FREQ	8.6	9.4	10.2	11.0	11.8	13.0	13.8	14.6	15.4	16.2	17.0
POL HH	0.5	-2.0	-2.2	-3.9	-4.7	-3.6	-3.9	-2.6	-2.3	-3.1	-3.9
POL VV	1.3	-1.3	-2.3	-3.5	-4.3	-4.0	-4.3	-4.2	-2.5	-3.7	-3.4

## ANTENNA ANGLE 10

FREQ	8.6	9.4	10.2	11.0	11.8	13.0	13.8	14.6	15.4	16.2	17.0
POL HH	-8.4	-8.4	-6.1	-8.6	-7.2	-6.8	-7.7	-7.7	-4.9	-6.9	-6.2
POL VV	-7.0	-8.2	-5.7	-7.0	-6.0	-5.4	-6.0	-5.2	-5.7	-6.6	-5.9

## ANTENNA ANGLE 20

FREQ	8.6	9.4	10.2	11.0	11.8	13.0	13.8	14.6	15.4	16.2	17.0
POL HH	-9.7	-10.0	-8.6	-7.5	-7.1	-7.9	-7.7	-7.9	-6.2	-7.7	-6.5
POL VV	-9.2	-9.5	-8.1	-7.7	-6.8	-6.2	-5.9	-5.8	-4.8	-6.1	-5.2

## ANTENNA ANGLE 30

FREQ	8.6	9.4	10.2	11.0	11.8	13.0	13.8	14.6	15.4	16.2	17.0
POL HH	-10.3	-9.9	-8.4	-9.0	-8.5	-8.3	-8.9	-7.4	-7.3	-7.2	-8.0
POL VV	-10.2	-9.9	-9.1	-7.6	-6.6	-5.9	-7.1	-5.8	-5.2	-6.5	-6.2

## ANTENNA ANGLE 40

FREQ	8.6	9.4	10.2	11.0	11.8	13.0	13.8	14.6	15.4	16.2	17.0
POL HH	-10.8	-11.4	-9.9	-9.5	-9.2	-8.9	-9.9	-7.8	-7.3	-9.0	-10.2
POL VV	-10.7	-10.4	-8.8	-8.4	-8.0	-7.8	-7.5	-7.1	-6.1	-7.5	-7.2

## ANTENNA ANGLE 50

FREQ	8.6	9.4	10.2	11.0	11.8	13.0	13.8	14.6	15.4	16.2	17.0
POL HH	-12.1	-12.8	-10.8	-11.1	-9.9	-10.7	-12.0	-10.7	-8.5	-10.7	-11.8
POL VV	-11.4	-11.9	-10.4	-10.5	-8.5	-8.2	-8.4	-7.3	-7.9	-9.2	-8.3

## ANTENNA ANGLE 60

FREQ	8.6	9.4	10.2	11.0	11.8	13.0	13.8	14.6	15.4	16.2	17.0
POL HH	-14.0	-13.9	-12.5	-12.6	-11.9	-11.7	-12.3	-11.8	-10.6	-12.2	-12.3
POL VV	-12.2	-13.0	-11.4	-11.0	-10.5	-9.9	-10.8	-9.4	-9.7	-11.5	-9.9

## ANTENNA ANGLE 70

FREQ	8.6	9.4	10.2	11.0	11.8	13.0	13.8	14.6	15.4	16.2	17.0
POL HH	-16.2	-16.2	-15.1	-14.2	-13.9	-13.3	-14.8	-13.5	-13.0	-14.3	-14.4
POL VV	-13.3	-13.8	-12.4	-12.3	-11.8	-11.4	-12.0	-10.9	-11.3	-12.6	-11.2

## ANTENNA ANGLE 0

FREQ	8.6	9.4	10.2	11.0	11.8	13.0	13.8	14.6	15.4	16.2	17.0
POL HH	-7.7	-7.2	-6.9	-6.9	-7.5	-6.7	-6.8	-7.0	-6.4	-7.7	-8.7
POL VV	-6.7	-7.9	-8.0	-7.9	-7.3	-6.3	-7.1	-6.3	-7.2	-8.8	-8.1

## ANTENNA ANGLE 10

FREQ	8.6	9.4	10.2	11.0	11.8	13.0	13.8	14.6	15.4	16.2	17.0
POL HH	-9.9	-9.7	-8.8	-10.2	-8.6	-8.8	-8.4	-8.6	-7.1	-9.1	-9.4
POL VV	-8.5	-9.9	-7.9	-8.0	-8.8	-7.2	-6.8	-6.6	-6.9	-8.3	-7.7

## ANTENNA ANGLE 20

FREQ	8.6	9.4	10.2	11.0	11.8	13.0	13.8	14.6	15.4	16.2	17.0
POL HH	-10.6	-10.7	-9.5	-9.1	-7.6	-9.2	-8.8	-8.4	-8.5	-9.1	-9.9
POL VV	-10.7	-9.7	-9.1	-8.9	-7.7	-7.2	-6.9	-6.9	-6.9	-9.3	-7.9

## ANTENNA ANGLE 30

FREQ	8.6	9.4	10.2	11.0	11.8	13.0	13.8	14.6	15.4	16.2	17.0
POL HH	-11.5	-11.9	-10.7	-10.1	-10.3	-9.6	-9.2	-9.0	-8.3	-9.3	-10.3
POL VV	-10.2	-9.8	-8.9	-8.6	-8.3	-8.0	-8.7	-6.6	-6.7	-9.0	-8.7

## ANTENNA ANGLE 40

FREQ	8.6	9.4	10.2	11.0	11.8	13.0	13.8	14.6	15.4	16.2	17.0
POL HH	-13.3	-12.2	-11.8	-11.8	-10.7	-10.7	-12.0	-11.0	-10.8	-11.6	-12.0
POL VV	-10.8	-10.8	-9.7	-10.0	-8.7	-7.5	-7.9	-7.6	-7.9	-10.6	-8.7

## ANTENNA ANGLE 50

FREQ	8.6	9.4	10.2	11.0	11.8	13.0	13.8	14.6	15.4	16.2	17.0
POL HH	-14.0	-13.7	-12.9	-12.5	-11.8	-11.9	-12.9	-12.8	-11.6	-12.9	-13.4
POL VV	-11.1	-11.0	-10.5	-10.2	-9.7	-9.2	-9.4	-8.9	-9.5	-10.8	-10.5

## ANTENNA ANGLE 60

FREQ	8.6	9.4	10.2	11.0	11.8	13.0	13.8	14.6	15.4	16.2	17.0
POL HH	-15.5	-15.1	-14.6	-14.0	-13.5	-13.7	-14.3	-13.8	-13.4	-14.9	-15.1
POL VV	-11.9	-12.2	-11.4	-11.3	-10.6	-10.6	-11.1	-10.4	-11.1	-13.1	-11.5

## ANTENNA ANGLE 70

FREQ	8.6	9.4	10.2	11.0	11.8	13.0	13.8	14.6	15.4	16.2	17.0
POL HH	-17.5	-17.4	-16.7	-16.0	-15.7	-15.7	-16.3	-15.6	-15.6	-16.5	-16.6
POL VV	-12.5	-13.0	-12.6	-12.5	-11.9	-12.0	-12.5	-12.2	-12.8	-14.6	-13.4



ORIGINAL PAGE IS  
OF POOR QUALITY

## ANTENNA ANGLE 0

FREQ	8.6	9.4	10.2	11.0	11.8	13.0	13.8	14.6	15.4	16.2	17.0
POL HH	-9.7	-9.0	-8.6	-8.6	-7.6	-6.2	-8.8	-8.3	-7.7	-7.5	-7.7
POL VV	-7.5	-8.2	-7.6	-8.1	-6.8	-6.2	-6.7	-4.7	-6.7	-7.6	-7.1

## ANTENNA ANGLE 10

FREQ	8.6	9.4	10.2	11.0	11.8	13.0	13.8	14.6	15.4	16.2	17.0
POL HH	-11.8	-10.3	-9.1	-8.9	-6.8	-7.7	-8.3	-8.2	-7.4	-8.6	-8.5
POL VV	-9.5	-9.1	-7.0	-8.8	-7.2	-6.4	-6.2	-6.2	-5.6	-7.8	-7.2

## ANTENNA ANGLE 20

FREQ	8.6	9.4	10.2	11.0	11.8	13.0	13.8	14.6	15.4	16.2	17.0
POL HH	-10.8	-10.6	-9.8	-8.9	-8.7	-7.5	-9.2	-8.3	-6.6	-8.9	-9.2
POL VV	-10.8	-9.6	-7.8	-8.6	-7.6	-6.5	-6.9	-6.3	-6.6	-8.4	-7.1

## ANTENNA ANGLE 30

FREQ	8.6	9.4	10.2	11.0	11.8	13.0	13.8	14.6	15.4	16.2	17.0
POL HH	-11.4	-11.1	-10.3	-9.1	-9.0	-9.1	-8.7	-8.0	-5.9	-9.7	-9.1
POL VV	-10.4	-10.6	-9.1	-8.9	-8.0	-6.7	-7.5	-7.2	-7.1	-9.0	-8.3

## ANTENNA ANGLE 40

FREQ	8.6	9.4	10.2	11.0	11.8	13.0	13.8	14.6	15.4	16.2	17.0
POL HH	-12.9	-12.4	-11.5	-11.1	-10.3	-10.4	-10.4	-10.0	-10.3	-11.5	-12.1
POL VV	-12.0	-12.0	-11.1	-10.8	-9.8	-8.2	-8.9	-8.2	-8.3	-10.2	-8.8

## ANTENNA ANGLE 50

FREQ	8.6	9.4	10.2	11.0	11.8	13.0	13.8	14.6	15.4	16.2	17.0
POL HH	-13.5	-13.2	-12.1	-12.0	-11.7	-10.7	-12.0	-10.4	-10.0	-12.0	-12.1
POL VV	-12.4	-12.4	-11.0	-11.1	-9.7	-9.2	-9.4	-9.3	-9.2	-10.6	-9.7

## ANTENNA ANGLE 60

FREQ	8.6	9.4	10.2	11.0	11.8	13.0	13.8	14.6	15.4	16.2	17.0
POL HH	-15.8	-15.0	-14.0	-13.0	-13.0	-12.0	-13.0	-12.0	-12.0	-13.0	-14.0
POL VV	-13.8	-13.8	-12.7	-12.6	-11.1	-10.9	-10.6	-10.2	-11.2	-12.0	-10.7

## ANTENNA ANGLE 70

FREQ	8.6	9.4	10.2	11.0	11.8	13.0	13.8	14.6	15.4	16.2	17.0
POL HH	-17.7	-16.9	-15.9	-15.2	-14.8	-14.1	-14.9	-14.0	-13.6	-15.0	-15.5
POL VV	-15.0	-14.6	-13.8	-13.4	-12.9	-12.1	-12.4	-11.6	-12.5	-13.6	-12.1

## ANTENNA ANGLE 0

FREQ	8.6	9.4	10.2	11.0	11.8	13.0	13.8	14.6	15.4	16.2	17.0
POL HH	-5.8	-7.1	-5.2	-4.3	-4.5	-5.6	-6.7	-5.2	-4.6	-5.2	-5.8
POL VV	-5.6	-7.2	-4.0	-4.7	-4.2	-4.9	-4.1	-4.1	-3.9	-4.7	-4.8

## ANTENNA ANGLE 10

FREQ	8.6	9.4	10.2	11.0	11.8	13.0	13.8	14.6	15.4	16.2	17.0
POL HH	-8.0	-8.2	-7.3	-7.4	-6.5	-6.6	-4.2	-6.7	-5.1	-7.3	-6.3
POL VV	-6.8	-6.8	-5.6	-7.5	-6.3	-5.4	-5.2	-4.0	-4.9	-7.1	-7.1

## ANTENNA ANGLE 20

FREQ	8.6	9.4	10.2	11.0	11.8	13.0	13.8	14.6	15.4	16.2	17.0
POL HH	-8.4	-9.0	-7.2	-8.2	-7.0	-5.7	-6.8	-6.3	-6.0	-7.3	-8.1
POL VV	-7.6	-8.6	-6.9	-5.6	-6.6	-5.6	-5.8	-4.9	-4.7	-6.8	-6.0

## ANTENNA ANGLE 30

FREQ	8.6	9.4	10.2	11.0	11.8	13.0	13.8	14.6	15.4	16.2	17.0
POL HH	-8.7	-8.8	-8.3	-7.2	-6.8	-6.9	-7.5	-6.7	-6.2	-9.1	-8.9
POL VV	-8.8	-8.4	-7.2	-7.2	-7.1	-5.7	-5.3	-5.5	-6.2	-7.4	-5.4

## ANTENNA ANGLE 40

FREQ	8.6	9.4	10.2	11.0	11.8	13.0	13.8	14.6	15.4	16.2	17.0
POL HH	-9.9	-10.3	-8.9	-7.5	-8.2	-7.3	-8.7	-8.1	-7.4	-9.3	-8.8
POL VV	-9.8	-8.9	-8.5	-7.6	-7.3	-6.5	-6.3	-5.9	-6.2	-7.2	-6.9

## ANTENNA ANGLE 50

FREQ	8.6	9.4	10.2	11.0	11.8	13.0	13.8	14.6	15.4	16.2	17.0
POL HH	-10.8	-10.4	-9.4	-9.6	-9.3	-8.3	-9.5	-8.6	-8.2	-10.6	-10.6
POL VV	-10.1	-10.8	-8.4	-9.4	-7.9	-7.8	-7.5	-6.5	-7.2	-8.3	-7.9

## ANTENNA ANGLE 60

FREQ	8.6	9.4	10.2	11.0	11.8	13.0	13.8	14.6	15.4	16.2	17.0
POL HH	-11.9	-11.6	-11.4	-10.6	-10.5	-10.6	-10.9	-10.2	-10.0	-11.6	-11.8
POL VV	-10.7	-10.7	-9.9	-9.5	-8.5	-8.4	-8.0	-7.6	-8.0	-9.3	-8.2

## ANTENNA ANGLE 70

FREQ	8.6	9.4	10.2	11.0	11.8	13.0	13.8	14.6	15.4	16.2	17.0
POL HH	-14.2	-13.8	-13.1	-12.9	-12.4	-11.9	-13.3	-11.9	-11.4	-13.2	-13.3
POL VV	-10.6	-10.6	-9.8	-10.2	-8.9	-9.2	-8.9	-8.3	-9.5	-10.6	-9.8

## Average Sigmao      Alfalfa, July 10, 1974

## ANTENNA ANGLE 0

FREQ	8.6	9.4	10.2	11.0	11.8	13.0	13.8	14.6	15.4	16.2	17.0
POL HH	2.2	0.7	2.1	1.5	3.4	2.7	1.5	3.1	4.6	2.0	1.1
POL VV	3.2	0.5	1.5	1.1	2.9	0.4	-0.5	1.8	2.5	1.2	1.7

## ANTENNA ANGLE 10

FREQ	8.6	9.4	10.2	11.0	11.8	13.0	13.8	14.6	15.4	16.2	17.0
POL HH	-8.3	-6.9	-7.0	-5.7	-7.2	-9.1	-7.8	-6.8	-6.9	-6.6	-7.2
POL VV	-7.2	-5.9	-6.7	-7.4	-7.6	-5.0	-5.5	-3.7	-6.6	-5.2	-6.3

## ANTENNA ANGLE 20

FREQ	8.6	9.4	10.2	11.0	11.8	13.0	13.8	14.6	15.4	16.2	17.0
POL HH	-9.3	-11.3	-9.1	-8.6	-8.8	-10.7	-8.8	-8.6	-5.7	-9.8	-9.7
POL VV	-9.1	-9.5	-8.9	-9.4	-10.2	-7.4	-9.0	-6.6	-7.0	-9.1	-7.6

## ANTENNA ANGLE 30

FREQ	8.6	9.4	10.2	11.0	11.8	13.0	13.8	14.6	15.4	16.2	17.0
POL HH	-10.7	-12.0	-9.7	-9.0	-9.9	-8.8	-6.9	-8.4	-8.1	-8.1	-9.4
POL VV	-9.8	-12.2	-10.7	-11.2	-11.0	-9.8	-7.7	-8.0	-8.1	-9.3	-8.8

## ANTENNA ANGLE 40

FREQ	8.6	9.4	10.2	11.0	11.8	13.0	13.8	14.6	15.4	16.2	17.0
POL HH	-13.2	-11.7	-11.3	-11.1	-11.5	-11.0	-10.4	-10.7	-9.8	-11.3	-11.4
POL VV	-12.4	-11.8	-11.6	-12.0	-10.3	-9.3	-9.9	-8.5	-9.2	-10.2	-9.4

## ANTENNA ANGLE 50

FREQ	8.6	9.4	10.2	11.0	11.8	13.0	13.8	14.6	15.4	16.2	17.0
POL HH	-12.9	-14.0	-13.3	-12.6	-12.8	-12.0	-12.2	-12.2	-11.1	-12.9	-12.7
POL VV	-13.0	-13.4	-12.3	-12.2	-11.8	-11.1	-10.8	-9.4	-10.5	-12.9	-10.1

## ANTENNA ANGLE 60

FREQ	8.6	9.4	10.2	11.0	11.8	13.0	13.8	14.6	15.4	16.2	17.0
POL HH	-13.0	-14.6	-14.4	-12.9	-13.9	-12.2	-13.2	-12.3	-12.0	-13.1	-13.1
POL VV	-13.3	-13.5	-13.2	-12.6	-12.0	-10.8	-11.6	-10.5	-11.3	-12.2	-10.2

## ANTENNA ANGLE 70

FREQ	8.6	9.4	10.2	11.0	11.8	13.0	13.8	14.6	15.4	16.2	17.0
POL HH	-15.3	-15.9	-15.1	-14.4	-13.9	-13.7	-14.9	-13.4	-13.5	-14.0	-13.6
POL VV	-14.1	-14.3	-13.3	-12.8	-12.3	-11.5	-11.8	-10.9	-11.5	-12.7	-11.3

## Average Sigmao      Alfalfa, July 17, 1974

## ANTENNA ANGLE 0

FREQ	8.6	9.4	10.2	11.0	11.8	13.0	13.8	14.6	15.4	16.2	17.0
POL HH	-6.2	-6.7	-5.2	-5.8	-5.8	-5.4	-6.0	-5.4	-5.6	-6.1	-5.1
POL VV	-3.7	-3.3	-3.3	-3.3	-3.4	-4.4	-3.9	-2.7	-3.4	-4.1	-4.1

## ANTENNA ANGLE 10

FREQ	8.6	9.4	10.2	11.0	11.8	13.0	13.8	14.6	15.4	16.2	17.0
POL HH	-11.7	-9.0	-7.9	-7.6	-5.6	-6.6	-8.2	-6.0	-6.9	-6.7	-6.7
POL VV	-9.7	-7.1	-7.4	-7.6	-5.7	-4.5	-5.7	-4.1	-4.7	-6.0	-6.0

## ANTENNA ANGLE 20

FREQ	8.6	9.4	10.2	11.0	11.8	13.0	13.8	14.6	15.4	16.2	17.0
POL HH	-12.0	-11.5	-10.1	-8.8	-7.9	-7.8	-8.1	-8.2	-7.3	-8.0	-8.0
POL VV	-10.3	-10.6	-9.5	-8.7	-7.3	-4.6	-6.6	-5.6	-6.3	-8.1	-8.1

## ANTENNA ANGLE 30

FREQ	8.6	9.4	10.2	11.0	11.8	13.0	13.8	14.6	15.4	16.2	17.0
POL HH	-12.1	-12.1	-9.8	-9.6	-8.8	-8.1	-9.0	-9.0	-6.6	-8.6	-8.6
POL VV	-11.5	-10.9	-8.9	-9.0	-8.1	-6.5	-7.5	-6.4	-5.4	-7.5	-7.5

## ANTENNA ANGLE 40

FREQ	8.6	9.4	10.2	11.0	11.8	13.0	13.8	14.6	15.4	16.2	17.0
POL HH	-12.4	-11.7	-11.4	-9.5	-10.2	-9.7	-10.1	-9.3	-8.8	-9.6	-9.6
POL VV	-10.9	-10.6	-9.9	-9.8	-7.7	-8.2	-7.7	-6.9	-7.1	-8.1	-8.1

## ANTENNA ANGLE 50

FREQ	8.6	9.4	10.2	11.0	11.8	13.0	13.8	14.6	15.4	16.2	17.0
POL HH	-14.0	-13.3	-12.4	-11.7	-11.6	-10.8	-11.4	-10.7	-9.7	-11.8	-11.8
POL VV	-12.5	-11.7	-10.3	-10.4	-9.2	-8.9	-8.7	-8.3	-8.8	-10.4	-11.4

## ANTENNA ANGLE 60

FREQ	8.6	9.4	10.2	11.0	11.8	13.0	13.8	14.6	15.4	16.2	17.0
POL HH	-14.9	-14.5	-13.7	-12.6	-12.4	-11.8	-12.4	-11.6	-11.1	-12.6	-12.6
POL VV	-12.9	-12.8	-11.1	-11.6	-10.3	-9.6	-9.6	-9.1	-9.8	-10.6	-10.6

## ANTENNA ANGLE 70

FREQ	8.6	9.4	10.2	11.0	11.8	13.0	13.8	14.6	15.4	16.2	17.0
POL HH	-13.2	-12.9	-11.9	-11.0	-10.5	-11.6	-10.7	-10.0	-10.7	-11.6	-11.0
POL VV	-11.0	-10.7	-10.4	-10.1	-9.9	-9.6	-10.1	-9.5	-9.6	-9.9	-9.9

## ANTENNA ANGLE 0

FREQ	8.6	9.4	10.2	11.0	11.8	13.0	13.8	14.6	15.4	16.2	17.0
POL HH	-7.2	-8.9	-8.4	-8.2	-7.3	-6.1	-7.3	-7.7	-5.7	-7.5	-6.5
POL VV	-6.2	-7.1	-6.3	-7.2	-6.1	-7.1	-5.7	-5.5	-4.6	-6.9	-5.1

## ANTENNA ANGLE 10

FREQ	8.6	9.4	10.2	11.0	11.8	13.0	13.8	14.6	15.4	16.2	17.0
POL HH	-9.7	-9.7	-7.7	-7.4	-7.2	-7.1	-6.8	-5.9	-4.6	-6.4	-7.0
POL VV	-8.7	-8.5	-7.2	-6.5	-5.7	-6.1	-5.2	-4.2	-3.8	-5.8	-5.3

## ANTENNA ANGLE 20

FREQ	8.6	9.4	10.2	11.0	11.8	13.0	13.8	14.6	15.4	16.2	17.0
POL HH	-10.7	-10.4	-9.5	-8.3	-8.6	-8.1	-6.7	-6.2	-4.8	-7.9	-7.5
POL VV	-9.2	-9.2	-8.2	-7.6	-6.4	-6.3	-5.2	-4.5	-4.8	-6.3	-5.6

## ANTENNA ANGLE 30

FREQ	8.6	9.4	10.2	11.0	11.8	13.0	13.8	14.6	15.4	16.2	17.0
POL HH	-11.1	-10.5	-10.0	-9.1	-8.2	-9.5	-8.5	-8.5	-7.0	-8.3	-8.9
POL VV	-9.8	-9.7	-8.7	-8.3	-7.8	-6.8	-5.7	-5.4	-5.2	-6.9	-5.3

## ANTENNA ANGLE 40

FREQ	8.6	9.4	10.2	11.0	11.8	13.0	13.8	14.6	15.4	16.2	17.0
POL HH	-11.8	-11.8	-11.4	-10.4	-9.7	-9.8	-10.3	-9.7	-8.8	-10.6	-10.4
POL VV	-10.9	-11.1	-9.4	-9.2	-7.6	-8.9	-8.4	-7.8	-7.4	-8.7	-7.2

## ANTENNA ANGLE 50

FREQ	8.6	9.4	10.2	11.0	11.8	13.0	13.8	14.6	15.4	16.2	17.0
POL HH	-13.5	-12.8	-12.2	-11.9	-11.9	-12.0	-12.1	-11.4	-10.0	-11.7	-11.3
POL VV	-12.2	-12.1	-10.9	-11.1	-10.1	-10.0	-9.8	-8.9	-8.8	-10.1	-9.0

## ANTENNA ANGLE 60

FREQ	8.6	9.4	10.2	11.0	11.8	13.0	13.8	14.6	15.4	16.2	17.0
POL HH	-15.3	-14.4	-13.6	-13.5	-13.0	-13.3	-13.6	-12.8	-12.5	-13.5	-13.4
POL VV	-12.4	-12.2	-11.5	-11.9	-11.1	-11.3	-10.3	-9.8	-9.8	-11.5	-10.0

## ANTENNA ANGLE 70

FREQ	8.6	9.4	10.2	11.0	11.8	13.0	13.8	14.6	15.4	16.2	17.0
POL HH	-17.4	-16.7	-15.8	-15.3	-14.8	-15.0	-15.0	-14.5	-13.9	-14.8	-14.7
POL VV	-14.2	-14.1	-13.2	-12.5	-12.1	-12.4	-11.6	-11.4	-11.7	-13.2	-11.5

## Average Sigmao      Alfalfa, August 13, 1974

## ANTENNA ANGLE 0

FREQ	8.6	9.4	10.2	11.0	11.8	13.0	13.8	14.6	15.4	16.2	17.0
POL HH	-5.7	-6.8	-6.4	-6.8	-6.3	-7.7	-6.8	-7.2	-4.2	-6.0	-4.3
POL VV	-5.4	-7.1	-7.2	-6.4	-5.0	-6.0	-3.9	-4.7	-3.8	-6.3	-5.4

## ANTENNA ANGLE 10

FREQ	8.6	9.4	10.2	11.0	11.8	13.0	13.8	14.6	15.4	16.2	17.0
POL HH	-8.9	-10.1	-8.4	-7.9	-7.3	-8.4	-7.6	-7.1	-5.8	-6.7	-6.1
POL VV	-5.3	-8.5	-7.2	-7.7	-5.7	-6.7	-4.9	-5.4	-4.8	-6.9	-5.2

## ANTENNA ANGLE 20

FREQ	8.6	9.4	10.2	11.0	11.8	13.0	13.8	14.6	15.4	16.2	17.0
POL HH	-9.6	-10.6	-8.8	-9.3	-8.8	-8.8	-8.4	-7.7	-6.6	-8.1	-8.9
POL VV	-8.3	-8.4	-7.6	-7.6	-7.0	-6.9	-6.0	-5.5	-5.7	-6.8	-5.5

## ANTENNA ANGLE 30

FREQ	8.6	9.4	10.2	11.0	11.8	13.0	13.8	14.6	15.4	16.2	17.0
POL HH	-10.7	-10.2	-10.0	-9.5	-9.1	-9.7	-9.4	-8.2	-7.2	-8.0	-8.2
POL VV	-8.1	-8.7	-8.6	-7.0	-8.2	-7.9	-7.1	-6.9	-5.7	-7.2	-6.6

## ANTENNA ANGLE 40

FREQ	8.6	9.4	10.2	11.0	11.8	13.0	13.8	14.6	15.4	16.2	17.0
POL HH	-11.8	-11.6	-10.5	-9.8	-9.9	-10.1	-10.2	-9.9	-8.3	-11.0	-10.1
POL VV	-9.3	-9.1	-8.5	-8.8	-8.7	-8.8	-8.5	-8.1	-7.3	-9.1	-7.4

## ANTENNA ANGLE 50

FREQ	8.6	9.4	10.2	11.0	11.8	13.0	13.8	14.6	15.4	16.2	17.0
POL HH	-12.6	-12.7	-11.9	-11.5	-11.0	-12.2	-11.6	-11.1	-10.3	-12.0	-12.0
POL VV	-12.6	-12.6	-11.9	-10.9	-10.6	-10.7	-10.2	-8.8	-9.3	-10.4	-8.7

## ANTENNA ANGLE 60

FREQ	8.6	9.4	10.2	11.0	11.8	13.0	13.8	14.6	15.4	16.2	17.0
POL HH	-14.6	-14.4	-13.8	-13.0	-12.5	-12.9	-12.6	-12.2	-11.1	-13.0	-12.8
POL VV	-12.4	-13.0	-12.4	-12.0	-11.2	-10.5	-9.9	-9.1	-9.7	-11.2	-9.3

## ANTENNA ANGLE 70

FREQ	8.6	9.4	10.2	11.0	11.8	13.0	13.8	14.6	15.4	16.2	17.0
POL HH	-16.2	-15.2	-15.2	-14.3	-14.5	-14.2	-14.5	-13.7	-13.2	-14.3	-13.8
POL VV	-12.8	-13.3	-12.6	-12.0	-11.6	-11.6	-10.7	-10.5	-10.6	-12.0	-10.1

## **CRINC LABORATORIES**

**Chemical Engineering Low Temperature Laboratory**

**Remote Sensing Laboratory**

**Flight Research Laboratory**

**Chemical Engineering Heat Transfer Laboratory**

**Nuclear Engineering Laboratory**

**Environmental Health Engineering Laboratory**

**Information Processing Laboratory**

**Water Resources Institute**

**Technical Transfer Laboratory**

**Air Pollution Laboratory**

**Satellite Applications Laboratory**

**CRINC**

